

Justification of ACI 446 Proposal for Updating ACI Code Provisions for Shear Design of Reinforced Concrete Beams

by Zdenek P. Bažant, Qiang Yu, Walter Gerstle, James Hanson, and J. Woody Ju

Due to a relatively large amount of experimental evidence and recent scientific advances, it is now generally recognized that, to ensure adequate safety margins, the size effect for designing reinforced concrete beams against shear failure must be incorporated into ACI code provisions. A purely empirical approach is impossible because the available test data, mostly obtained on small beams, need to be extrapolated to much larger beams for which tests are scant or nonexistent. Arguments for an improved code formulation are summarized, and verification by a database compiled by Joint ACI-ASCE Committee 445 is reviewed.

Keywords: shear failure; size effect; reinforced concrete.

INTRODUCTION

ACI 318-05, Eq. (11-3), currently specifies the contribution of concrete to the cross section shear strength of reinforced concrete members as $V_c = 2\sqrt{f'_c} b_w d$ (valid in psi, lb, and in.), where f'_c is the required compression strength of concrete, d is the beam depth from the top face to the longitudinal reinforcement centroid, and b_w is the web width. This code formula was justified on the basis of a Joint ACI-ASCE Committee database,¹ which involved only small beams of average depth 13.4 in. (340 mm). This formula was set not at the mean of these data but near their lower margin, at a level that appears to be the 5% fractile (or probability cutoff) of the data if a Gaussian distribution is fitted to the data (refer to Fig. 1).

The code formula gives a size-independent average concrete shear strength, $v_c = V_c/b_w d$ (identical to the nominal strength in mechanics terminology). Compelling experimental evidence for size effect, however, has been gradually accumulated since 1962,²⁻⁴ and some large-scale tests, particularly those in Tokyo⁵⁻⁷ and in Toronto⁸⁻¹¹ showed the urgency of taking into account the size effect. Furthermore, recent analysis of some major structural disasters (for example, the Sleipner oil platform; a warehouse at Wilkins AF Base in Shelby, Ohio; and the Koror box girder bridge in Palau) indicated that the size effect must have been a contributing factor (and so it seems to have been for the overpass failure in Laval, Quebec, on September 29, 2006). A base of 296 data assembled at Northwestern University² and a recent larger database of 398 data compiled by ACI Subcommittee 445F (refer to Fig. 2 and 3), clearly show the current code to be unconservative for large beams. Especially, a large (6.2 ft [1.89 m] deep) and lightly reinforced concrete beam has been observed to fail at a load less than 1/2 of the required design strength V_u/ϕ (with ϕ from ACI 318-05).

The purpose of this paper is to summarize the justification of a revision¹² of Section 11.3 of ACI 318-05 (detailed arguments are presented separately^{13,14}).

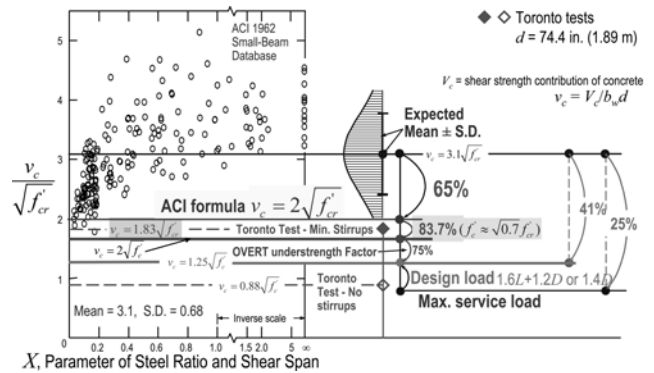


Fig. 1—Joint ACI-ASCE Committee 326¹ small beam database used to justify current ACI code formula for shear force capacity V_c due to concrete in reinforced concrete beams with and without stirrups, and reductions specified or implied by ACI 318-05 that were justified by this database ($f'_c =$ average compression strength of concrete from tests; $f'_c \approx 0.7f'_{cr} =$ required concrete strength, as defined in ACI 318-05).

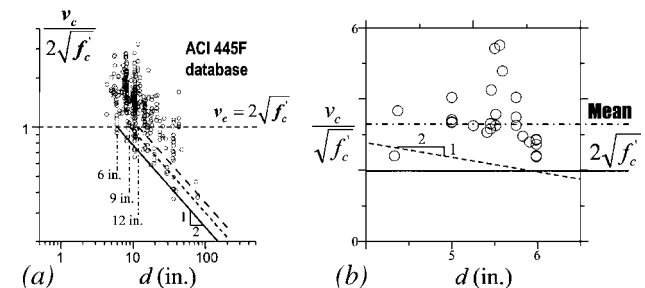


Fig. 2—Alternative simplified size effect formula compared with: (a) complete ESDB; and (b) small-size portion of that database in expanded scale.

RESEARCH SIGNIFICANCE

To make the risk of structural failure much smaller than various inevitable risks that people face, the tolerable failure probability is approximately one in 1 million.¹⁵ This value agrees with experience for small beams, but not for large ones, for which it has been approximately one in 1000^{16,17} (and could become one in 100 or higher as ever larger beams are built). Whether or not such intolerable risk will have to be tolerated depends largely on taking the size effect properly into account. This is an issue of paramount significance.

ACI Structural Journal, V. 104, No. 5, September-October 2007.
MS No. S-2006-186 received May 5, 2006, and reviewed under Institute publication policies. Copyright © 2007, American Concrete Institute. All rights reserved, including the making of copies unless permission is obtained from the copyright proprietors. Pertinent discussion including author's closure, if any, will be published in the July-August 2008 ACI Structural Journal if the discussion is received by March 1, 2008.

ACI member **Zdenek P. Bazant** is the McCormick School Professor and W.P. Murphy Professor of Civil Engineering and Materials Science at Northwestern University, Evanston, Ill. He is a member of ACI Committees 209, Creep and Shrinkage in Concrete; 348, Structural Safety; and 446, Fracture Mechanics; and Joint ACI-ASCE Committees 334, Concrete Shell Design and Construction; 445, Shear and Torsion; and 447, Finite Element Analysis of Reinforced Concrete Structures.

Qiang Yu is a Graduate Research Assistant and Doctoral Candidate at Northwestern University.

ACI member **Walter Gerstle** is a Professor in the Department of Civil Engineering at the University of New Mexico, Albuquerque, N.Mex. He is a member of ACI Committee 446, Fracture Mechanics, and Joint ACI-ASCE Committee 447, Finite Element Analysis of Reinforced Concrete Structures.

ACI member **James Hanson** is an Assistant Professor at Rose-Hulman Institute, Terre Haute, Ind. He is a member of ACI Committees 440, Fiber-Reinforced Polymer Reinforcement; 446, Fracture Mechanics; E802, Teaching Methods and Educational Materials; and E803, Faculty Network Coordinating Committee.

ACI member **J. Woody Ju** is a Professor and Chair of the Department of Civil Engineering, University of California-Los Angeles, Los Angeles, Calif. He is a member of ACI Committees 201, Durability of Concrete; 228, Nondestructive Testing of Concrete; 446, Fracture Mechanics; and E803, Faculty Network Coordinating Committee.

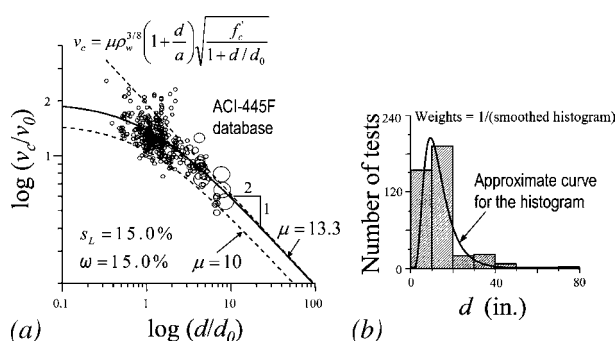


Fig. 3—(a) Comparison of proposed formula with ESDB; and (b) smoothing of histogram of beam depth in ESDB.

EXPERIMENTAL DATABASE USED

Thousands of experiments have been conducted around the world to assess the shear capacity of concrete members, although only a small fraction of them were specifically aimed at the effect of size. ACI Subcommittee 445F extracted, from a collection of more than 1000 data, a new database of 398 data, called the Evaluation Shear Database (ESDB).¹⁸ Only beams with no shear reinforcement, subjected to three-point or four-point loading, are included. All the beams have a rectangular cross section except that 24 are T-beams. The beam depth ranged from 4.33 to 78.74 in. (110 to 2000 mm) (with a mean of 13.6 in. [345 mm], which is nearly equal to the mean of 13.4 in. (340 mm) in the 1962 database, and a coefficient of variation [CoV] of 74%); the shear-span ratio (a/d) (with $a = M/V$) ranged from 2.41 to 8.03 (with a mean of 3.6 and a CoV of 26%); the compression strength f_c' of concrete of the beams ranged from 1828 to 16,080 psi (12.6 to 110.9 MPa) (with a mean of 6104 psi [42.09 MPa] and a CoV of 55%); the longitudinal steel ratio ranged from 0.14 to 6.64% (with a mean of 2.3% and a CoV of 52%); and the maximum aggregate size, known for only for 341 data points, ranged from 0.25 to 1.5 in. (6.35 to 38 mm) (with a mean of 0.71 in. [18 mm] and a CoV of 40%).

The ESDB has been adopted for the present studies in ACI Committee 446, even though the rationality and impartiality of the criteria used to select the data have been questioned.¹⁹⁻²³ For instance, the largest beams ever tested, up to 9.84 ft (3 m) deep⁵⁻⁷ were excluded from the ESDB based on the fact that they were subjected to distributed load, a combination

of which, with point loads in the same database, was thought to complicate interpretation. But this position disregards the fact that the code provision must apply to both. The reduced-scale beam tests at Northwestern University,⁴ with an aggregate size of 0.19 in. (4.8 mm) and a beam width b_w of 1.90 in. (48 mm), were excluded with the explanation that, inexplicably, only beams with b_w greater than 1.97 in. (50 mm) were admissible; these tests, however, exhibited the most systematic size effect trend, had an exceptionally broad size range (1:16), and achieved the highest brittleness number²⁴ among all the available tests, thus mimicking the brittleness of very large beams (b_w equaled 10 maximum aggregate sizes in these tests, which is not only adequate but also, after a width increase by mere 4%, would have technically qualified these data for inclusion in the ESDB; the width increase would not have distorted interpretation because it is generally accepted that the effect of beam width on v_c is nil^{8,20-23} if the width exceeds approximately four aggregate sizes).

While the size effect is of major concern for beams deeper than approximately 40 in. (1 m), 86% of the tests in the ESDB pertain to beam depths less than 20 in. (0.5 m), 99% less than 43 in. (1.1 m), and 100% less than 79 in. (2 m) (see the database histogram in Fig. 1 of Reference 13). The CoV or ω of the deviations of an empirical size effect formula derived directly from the ESDB will therefore be totally dominated by small size beams for which the size effect is unimportant. Thus, it is possible that some formula that gives the lowest ω for the ESDB could be completely wrong for large sizes while another formula that might give a higher ω could be much more realistic for large sizes. Obviously, a purely empirical extrapolation to large sizes cannot be trusted. A solid scientific basis is crucial. In the plot of $\log(v_c/\sqrt{f_c'})$ versus $\log d$ (refer to Fig. 2 in Reference 13) it is striking that, while the curves of various previously proposed formulas are very different, they all appear to be equally good (or equally bad) compared with the ESDB. The reasons are: 1) The size range covered by the database is not broad enough; 2) the scatter is enormous because the effects of concrete strength and type, longitudinal steel ratio, shear span, and aggregate size are not separated by a suitable choice of relevant regression variables; and 3) the ESDB database is biased by the fact that the interval averages of other influencing variables (ρ_w , a/d , f_c'), as well as the spread between the minimum and maximum interval values of each variable, vary strongly from one size interval to the next.

A serious obstacle to extracting a size effect formula purely empirically from the ESDB is the fact that the vast majority (more than 97%) of its 398 data points come from tests motivated by different objectives (such as the effect of concrete type, reinforcement, and shear span), in which the beam depth was varied only slightly or not at all. The effects of variables other than d exhibit enormous scatter, which masks the size effect trend. It is necessary to find regression coordinates that include the effects of influencing variables other than the size.

CHOICE OF BASIC SIZE EFFECT FORMULA

In view of the preceding arguments, it is necessary to establish the beam shear formula in two steps: 1) select the form of the formula on the basis of a sound theory and verify it by close fits of the available individual test series with geometrical scaling and a sufficiently broad size range; and 2) calibrate the selected formula using the whole ESDB. This procedure¹²⁻¹⁴ led to the classical energetic size effect formula²⁵

$$v_c = \frac{v_0}{\sqrt{1 + d/d_0}} \quad (1)$$

The first step shows that the choice of the form of size effect would not be contaminated by random variation of parameters other than size d . Because of high random scatter in beam shear tests, the size range should be at least 1:8 to obtain a clear size effect trend. Two data sets that closely approach these requirements are those obtained at Northwestern University (not included in the ESDB) and the University of Toronto (refer to Fig. 4), which shows that the fits by Eq. (1) are very close.

The salient property of this formula is that, for large sizes, it approaches an inclined asymptote of slope $-1/2$ in a doubly logarithmic plot, corresponding to a power law of the type $d^{-1/2}$. This property, which was endorsed as essential by a unanimous vote of ACI Committee 446 in Vancouver in 2003, is indeed verified by the available broad-range test series—Northwestern University tests (Fig. 4(a)), University of Toronto tests (Fig. 4(b)), and the record-size Japanese tests (Fig. 4(c) and (d)). It is not contradicted by any of the existing additional seven test series of a lesser but still significant size range^{8,26,27} (refer to the plots in Reference 14).

The Japan Society of Civil Engineers (JSCE) pioneered the size effect for design code long ago. It adopted a power-law, $v_c \propto d^{-1/4}$, which was proposed by Okamura and Higai²⁸ already in 1980 before the energetic size effect was discovered and was motivated by the Weibull statistical theory, at a time when this classical theory was the only theory of size effect. A decade later it became clear that the Weibull theory applies only for structures failing right at the initiation of fracture growth from a smooth surface,^{29,30} which is not the case for reinforced concrete beams, where a large crack or cracking zone develops before the maximum load is reached.^{24,29-32} Besides, even if the Weibull statistical theory were the right explanation for the JSCE power law, its exponent would need to be changed from $-1/4$ to $-1/12$. The reason is twofold: 1) a realistic Weibull modulus for concrete is 24 rather than 12^{14,33}; and 2) the fracture scaling must be considered two-dimensional ($n = 2$) because, in not too wide beams, the fracture must (for reasons of mechanics) grow over the whole beam width nearly simultaneously. But the exponent $-1/12$ would be far too small to describe the strong size effect evidenced by test data, including those of JSCE.

The formula based on the crack spacing according to the modified compression field theory (MCFT) has the opposite problem of the JSCE formula. Its large-size asymptote is $v_c \propto d^{-1}$, while the exponent of the greatest thermodynamically possible magnitude is $-1/2$ (or else the energy flux into moving fracture front would be infinite^{24,29,31}). Besides, the proposed justification of the MCFT formula³⁴ is unrealistic for two reasons^{13,14}: 1) crack spacing is not uniquely related to energy release and depends also on other factors³⁵; and 2) the crack-bridging tensile and shear stresses at maximum load are reduced to almost zero while the failure is caused mainly by near-tip compression stresses parallel to the diagonal shear crack. As for the CEB-FIP formula, it is purely empirical and thus cannot be trusted for large sizes for which data are scant or nonexistent.

The deceptiveness of a purely empirical power-law extrapolation of a combined database such as ESDB is illustrated in Fig. 5(a), (b), and (c). Suppose that the mean

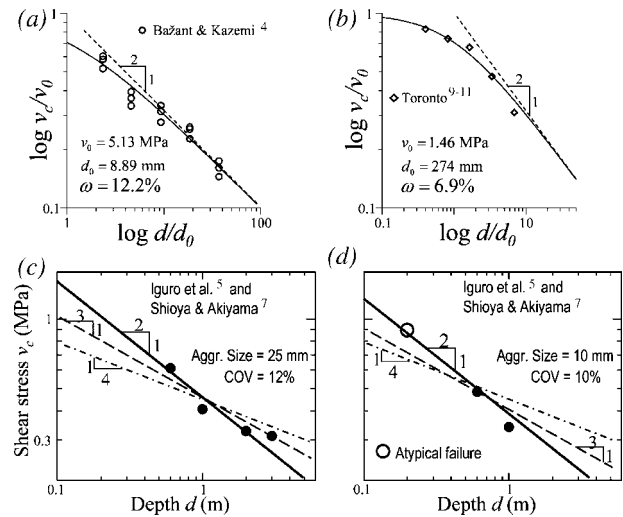


Fig. 4—Comparison of size effect Formula (1) to beam shear test series with greatest size range and with nearly geometrical scaling: (a) microconcrete beams tested by Bažant and Kazemi at Northwestern University in 1991⁴ (not included in ESDB); (b) large size tests at University of Toronto reported by Podgorniak-Stanik⁹ and Lubell et al.,¹¹ and (c) and (d) large beams under uniform loading in Tokyo.⁵⁻⁷

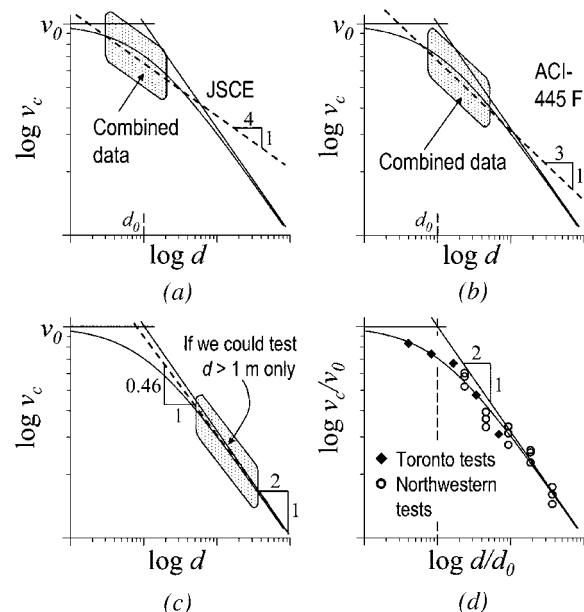


Fig. 5—Example of effect that choice of size range of highly scattered tests can have on regression result when straight line plot in log-scale is assumed.

size effect trend agrees perfectly with size effect Law (1), but different investigators choose different size effect ranges for testing. In view of scatter, each of them fits a power law to his data. The exponents of this power law will vary between 0 and $-1/2$ depending on the chosen size range. An unambiguous, purely experimental verification of Eq. (1) would require a very broad size range (Fig. 5(d)).

STATISTICAL CALIBRATION, VERIFICATION, AND EVALUATION OF PROPOSED FORMULA

The next step is to calibrate the size effect formula by proper statistical regression. Let \bar{v}_i ($i = 1, 2, \dots, n$) be the

measured data points for sizes d_i and let v_i be the corresponding values of v_c calculated from the proposed formula. It turns out that the right approach is not to minimize the sum of squared errors (or residuals) $\sum_i (v_i - \bar{v}_i)^2$ because the variance of the data (precisely, conditional variance $\text{Var}(v_c|d)^{36}$) is heteroscedastic, that is, strongly decreases with the increasing size d . To minimize statistical bias, the statistical variable v_c should be transformed so as to make the variance, and thus the scatter band width, approximately uniform,³⁶ or homoscedastic. This is approximately achieved by the transformation $y = \ln v_c$. Thus, the objective of data regression is to minimize, in the scale of $\ln v_c$, the square of the standard error of regression s_L , the unbiased definition of which is $s_L^2 = \sum_{i=1}^n \ln(v_i/\bar{v}_i)^2 / (n-p)$ where p is the number of free parameters in data fitting (because $(d \ln v_c)^2 = (dv_c)^2 / v_c^2$), the transformation from v_c to y has a similar effect as applying weights proportional to $1/v_c^2$. In the linear scale of v_c , the corresponding CoV of regression is $\omega = (e^{s_L} - e^{-s_L})/2$ (which herein is almost equal to s_L).

According to the ACI code, the factored shear force V_u must not be greater than $\phi(V_c + V_s)$ where $\phi = 0.75$ is the understrength (strength reduction) factor and V_s is the yield shear force carried by shear reinforcement. The maximum shear force V_c that can be carried by concrete is proposed to be calculated as¹⁴

$$V_c = 10b_w \rho_w^{3/8} \left(1 + \frac{d}{a}\right) \sqrt{\frac{f'_c d_0 d}{1 + d_0/d}}, \quad d_0 = \kappa f'_c{}^{-2/3} \quad (2)$$

where, if d_a is known, $\kappa = 3800 \sqrt{d_a}$; if not, $\kappa = 3330$ (3)

where V_c is in lb, f'_c is in psi, ρ_w is the longitudinal steel ratio, and b_w and d are in inches. The expression for d_0 is empirical. Note that V_c increases continuously with d , but less than proportionately (because of size effect).

As seen in Fig. 2(b), for very small d , the V_c value according to the proposed Formula (2) is greater than predicted by the current Formula (4), $V_c = 2 \sqrt{f'_c} b_w d$. This means that the current formula can be used safely within a certain range. The permissible safe range for Eq. (4) is $d \leq 6$ in. (150 mm). This is ascertained from the ESDB plotted in Fig. 2, which reveals that for $d \leq 6$ in. (150 mm), no beam test gave a shear strength less than the value given by Eq. (4).

As a simple and safe (though often uneconomical) alternative (Fig. 2(a)), the simple formulas

$$\text{for } d \leq 6 \text{ in. (150 mm): } V_c = 2b_w \sqrt{f'_c} d \quad (4)$$

$$\text{for } d > 6 \text{ in. (150 mm): } V_c = 5b_w \sqrt{f'_c} d \quad (5)$$

can be used instead of Eq. (2). In Fig. 2, the solid inclined line represents Eq. (5). Note that if the small size limit were set at 9 or 12 in. (0.23 or 0.3 m), as shown by the other two dashed inclined lines, the design equation would not be safe.

Formula (2), as well as Formulas (4) and (5), are recommended for use regardless of whether or not there is shear reinforcement. For small beams, shear reinforcement appears to increase V_c appreciably. But this observation is based on only one large beam test, which is statistically insufficient, and the test shows that the size effect is only mitigated, but

not eliminated, by shear reinforcement. Furthermore, finite element simulations at Northwestern University (based on nonlocal damage concept) show that, for large beams exceeding approximately 60 in. (1.52 m) in depth, shear reinforcement does not increase V_c and does not help against size effect. For very deep beams with strong shear reinforcement, these simulations indicate that not only is V_c not increased, but V_s at maximum load is much below the yield strength of stirrups $V_s = A_s f_y d/s$.

The general form of Formula (1) has been verified for many different structural geometries and many different quasibrittle materials. The analytical derivations (though not the numerical verifications) have been subjected to the hypothesis that a large crack or long band of cracking damage develops in a stable manner before the maximum load is reached and the failure modes of small and large structures are geometrically similar (experiments as well as finite element simulations document that this is approximately true for beam shear failures).

The current ACI code also involves corrections to the expression for V_c due to simultaneous action of compressive or tensile axial force, and for the calculation of the shear span ratio from the bending moment in the presence of axial force. The multiplicative factors for these corrections are applied to the present formula with no change.

The expressions for the parameters in Eq. (2) through (5) have been obtained by simplified mechanical considerations and calibrated by optimization of data fits.¹⁴ The least-square fitting of the data, conducted in the plot of $\ln v_c$ versus $\ln d$, was a weighted regression. The weighting was necessary to counteract the subjective bias due to crowding of the data points in the small-size range; refer to Fig. 3 where the data points are represented by circles having areas proportional to the weight. A logarithmic scale of d needs to be used because, for example, the size effect from 11.8 in. (0.3 m) to 11.8 + 11.8 in. (0.3 + 0.3 m) is significant, but from 118 in. (3 m) to 118 in. + 11.8 in. (3 m + 0.3 m) insignificant. The optimum data fitting was accomplished by a standard library subroutine for the Levenberg-Marquardt nonlinear optimization algorithm. The heavy solid line in Fig. 3 represents the mean fit formula, and the dashed line represents the design formula, which is set at the lower 5% fractile of the scatter band width. The overall CoV or ω of the errors of Formula (2) calculated by the ESDB is 15%. The CoV of the errors for various size intervals of 10 in. (0.25 m) width are 18.8, 15.6, 11.6, 15.3, 14.5, and 15.7%, respectively (note that these values are approximately uniform, which conforms homoscedasticity, is required for a proper statistical approach and is achieved by transforming the regression variable from v_c to $\ln v_c$).

The reason why Eq. (3) gives two options for calculating d_0 is that sometimes the design needs to be made before the maximum aggregate size d_a has been decided. Both expressions for d_0 give the same value when $d_a = 0.77$ in. (≈ 20 mm).

REGRESSION OF DATA GROUPED IN EQUAL-RATIO INTERVALS

To minimize the size effect bias due to highly nonuniform distribution of data through the size range of interest, subdivide the range of beam depths d of the existing test data into five size intervals (Fig. 6). They range from 3 to 6 in. (76.2 to 152.4 mm), from 6 to 12 in. (152.4 to 304.8 mm), from 12 to 24 in. (304.8 to 609.6 mm), from 24 to 48 in. (609.6 to 1219.2 mm), and from 48 to 96 in. (1219.2 to 2438.4 mm).

Note that the borders between the size intervals are chosen to form a geometric (rather than arithmetic) progression because what matters for size effect is the ratio of sizes, not their difference (note that, for example, from $d = 4$ to 24 in. [100 to 600 mm], the size effect is strong and from 400 to 420 in. [10,160 to 10,668 mm], the size effect is negligible).

To filter out the effect of influencing parameters other than d , each interval of d must include only the data within a certain restricted range of ρ_w values such that the average $\bar{\rho}_w$ will be almost the same for each interval of d . Similarly, the range of a/d and d_a must be restricted so that the average $\bar{a/d}$ and \bar{d}_a be approximately the same for each interval of d . Because, as generally agreed, the effect of the required concrete strength f'_c is adequately captured by assuming the shear strength of cross section v_c to be proportional to $\sqrt{f'_c}$, the range of f'_c does not need to be restricted and the ordinate \bar{y} of data centroid in each interval may be obtained by averaging, within that interval, not the v_c values but the values of $y = v_c/\sqrt{f'_c}$ that fall into the aforementioned restricted ranges of ρ_w , a/d , and d_a .

As shown in Fig. 6, there are only three test data in the size interval 48 to 96 in. (1219 to 2438 mm), one of which has the longitudinal steel ratio of $\rho_w = 0.14\%$, the second is 0.28%, and the third is 0.74%. This extremely low ρ_w makes it impossible to find similar data in other intervals of d . For example, the minimum ρ_w is 0.91% within the first interval of d , and 0.46% within the third interval. Therefore, one may consider the size range from 3 in. (76 mm) to only 48 in. (1219 mm). After searching the ESDB, there are 7, 19, 25, and 36 data points within the admissible ranges for each interval of d (ideally, the number of data in each interval should be the same, and thus it is impossible to eliminate bias completely). For these restricted ranges, the mean values of ρ_w are 1.51%, 1.5%, 1.51%, and 1.5%; the mean values of a/d are 3.44, 3.25, 3.25, and 3.21, respectively; and the mean values of d_a are 0.66, 0.66, 0.68, and 0.65 in. (16.8, 16.8, 17.3, and 16.5 mm). Thus, data samples with minimum bias in terms of ρ_w , a/d , and d_a are achieved (a systematic computerized procedure toward this end is developed in Reference 37). The data centroids for each interval are plotted as the diamond points in the plot of $\log(v_c/\sqrt{f'_c})$ versus $\log d$ (Fig. 6(a))—on top they are shown together with all the data points of the database, and at bottom they are shown alone. Despite enormous scatter in the database (Fig. 6(a)[top]), the trend of these centroids is quite systematic.

Assuming the statistical weight of each size interval centroid in Fig. 6 to be the same, statistical regression is used to obtain the optimum least-square fit of these four centroids with the theoretically justified size effect law $v_c/\sqrt{f'_c} = C(1 + d/d_0)^{-1/2}$, where C and d_0 equal the free constants to be found by the fitting algorithm. The fit is seen to be good; it has a very small CoV of errors ($\omega = 2.7\%$), and the asymptotic slope $-1/2$ required by fracture mechanics^{2,13,14,25} is seen to match the data trend well.

To increase the size range, consider now that one point from the largest size interval from 48 to 96 in. (1219 to 2438 mm), namely the Toronto beam with $\rho_w = 0.74\%$, is included; refer to Fig. 6 (admittedly, one data point is too few, but that is what must be accepted because of the cost of testing very large beams). Then the same procedure is followed as previously mentioned and, for the other four intervals of d , 1, 2, 4, and 15 data points are found for which the means of ρ_w in the interval of d are 0.91, 0.94, 0.92, 0.91, and 0.74%, while the mean of $a/d = 2.9$ and the mean maximum aggregate size $d_a = 0.39$ in. (10 mm) are the same

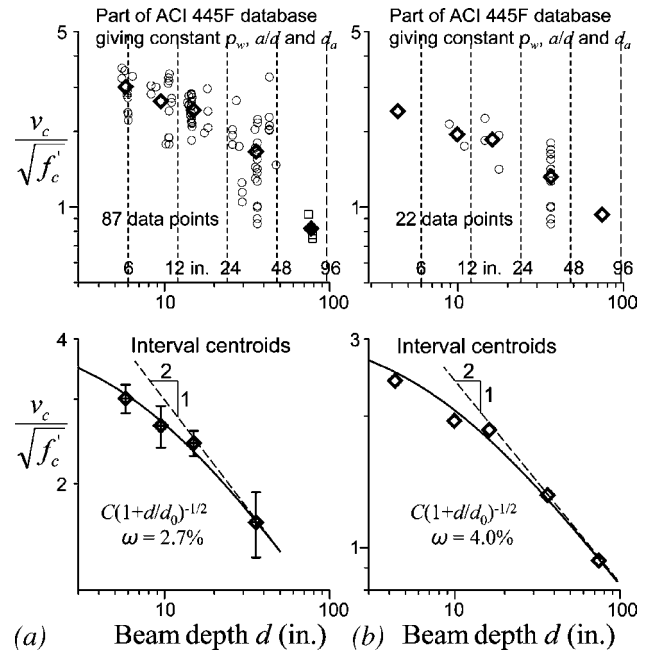


Fig. 6—ACI-ESDB and statistical regression of centroids of test data with intervals of equal width: (a) large-size interval not included; and (b) all intervals included.

for each interval. Again, the size effect trend is very clear, and agrees well with the asymptotic slope of $-1/2$. The CoV of errors is now $\omega = 4\%$.

The foregoing regression with minimized statistical bias lends no support for the previously proposed power laws $v_c/\sqrt{f'_c} = Cd^{-1/4}$ or $Cd^{-1/3}$. Neither does it lend any support to the asymptotic size effect $v_c/\sqrt{f'_c} = Cd^{-1}$ implied by an alternative model based on MCFT (an exponent magnitude greater than 0.50 is energetically as well as statistically impossible.^{24,29,31}

EXCESSIVE FAILURE PROBABILITY CAUSED BY IGNORING SIZE EFFECT

Could the size limit of 6 in. (150 mm) in Eq. (4) be extended to 39.4 in. (1 m), as suggested by some researchers? No. To demonstrate it,³⁸ the data in the size range of d from 4 to 12 in. (101.6 to 304.8 mm), centered at 8 in. (203.2 mm), are isolated from the database (Fig. 7(a)). Within this narrow range, no size effect trend is discernible, and the data may be treated as a statistical population. Its mean and CoV are found to be $\bar{y} = \bar{v}_c/\sqrt{\bar{f}'_c} = 3.2$ and $\omega = 25\%$ (this relatively high value of ω is the consequence of variability of many parameters in the database). The data in this range suffice to fix the probability density distribution function (pdf) for this range, which is assumed to be log-normal. The same pdf is compared in Fig. 7(a) with the series of individual tests of beams of various sizes made at the University of Toronto, which have been invoked by some engineers to claim that the size effect may be ignored for d up to 39.4 in. (1 m).

It should be noted that, for the type of concrete, steel ratio, and shear span ratio used in the Toronto tests, their shear strength value lies (in the logarithmic scale) at a certain distance a below the mean of the pdf. Because the width of the scatter band in Fig. 7(a) in logarithmic scale does not vary appreciably with the beam size, the same pdf and the same distance a between the pdf mean and the Toronto data must be expected for every beam size d , including the sizes

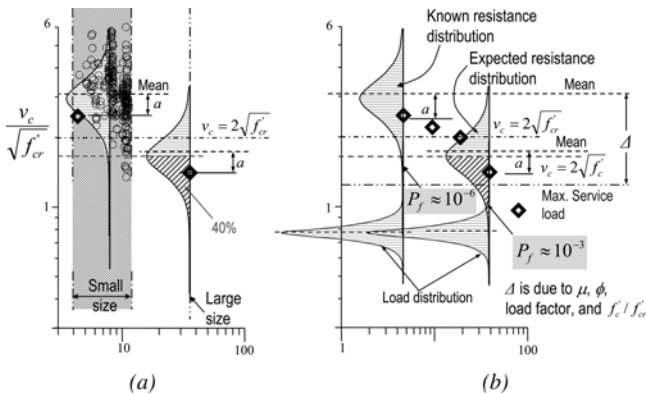


Fig. 7—(a) Probability distribution of shear strength of beams from 3.94 and 11.81 in. (10 to 30 cm) deep, based on ACI Committee 318-F database, compared with Toronto data; and (b) failure probability for small beam and 3.28 ft (1 m) deep beam.

of $d = 39.4$ and 74.4 in. (1 and 1.89 m) for which there is only one data point. In other words, if the Toronto test for $d = 39.4$ in. (1 m) were repeated for many different types of concrete, steel ratios, and shear span ratios, humidity and temperature conditions, etc., one would obtain a pdf shifted downwards, as shown in Fig. 7(a). According to the log-normal pdf shown, the proportion of unsafe 39.4 in. (1 m) deep beams would be approximately 40%, while for small beams, it is only 1%. This is intolerable. A design code known to have such a dangerous property is unacceptable.

More seriously, a design code ignoring the size effect for beams of $d < 39.4$ in. (1 m) will cause the failure probability P_f of 39.4 in. (1 m) deep beams to be approximately 1000 times larger than that of small beams 8 in. (200 mm) deep. To demonstrate it, consider the pdf of the extreme loads expected to be applied on the structure, which is denoted as $f(y)$. Based on the load factor of 1.6 and the understrength factor of $\phi = 0.75$, the mean of the pdf of the extreme loads will be positioned as shown in Fig. 7(b). Assuming the individual loads to have the log-normal distribution, their pdf is as shown in Fig. 7(b). Based on the CoV of extreme loads, herein assumed as $\omega_L = 10\%$, the failure probability may now be calculated from the well-known reliability integral^{36,39,40}

$$P_f = \int_0^{\infty} f(y)R(y)dy \quad (6)$$

where $R(y)$ is the cumulative probability density distribution (cdf) of structural resistance. Upon evaluating this integral

$$\text{for beams of 8 in. (200 mm) depth, } P_f \approx 10^{-6} \quad (7)$$

$$\text{for beams of 39.4 in. (1 m) depth, } P_f \approx 10^{-3} \quad (8)$$

The failure probability of one in 1 million corresponds to what the risk analysis experts generally consider as tolerable,¹⁵⁻¹⁷ but one in 1000 is intolerable.

SIZE EFFECT ON CONCRETE CONTRIBUTION V_c TO SHEAR STRENGTH OF BEAMS WITH STIRRUPS

Some researchers have recently voiced the opinion that shear failure of beams with minimum or heavier shear

reinforcement exhibits no size effect. This opinion seemed to be reinforced by one recent test at the University of Toronto.¹¹ In this test, a beam 74.41 in. (1.89 m) deep, with approximately minimum stirrups, supported a shear force V exceeding the required nominal shear strength V_u/ϕ by 6% that is calculated according to ACI 318-05 (this observation was claimed to confirm safety, even though this test result is, in fact, 11% less than required if one notes that the design should be based on the required compression strength, that is, on $v_c = 2\sqrt{f'_c}$, rather than the average compression strength, that is, on $v_c = 2\sqrt{f'_{cr}}$).

A proper statistical analysis, however, reveals that this conclusion is incorrect. The correct interpretation of the Toronto test is that there is a size effect, and that the reduction of V_c caused by size effect is, for the Toronto test, approximately 41%, which is quite significant, though still much less than the 76.2% reduction observed in a companion beam without stirrups.⁴¹ The reason is that, aside from the (overt) understrength factor $\phi = 0.75$, the shear design implies two covert understrength factors:

- Material understrength factor $\phi_m \approx \sqrt{0.7}$, due to the fact⁴¹ that the design must be based not on f'_{cr} but on f'_c , which represents, on the average, approximately 70% of f'_{cr} ; and
- Understrength factor ϕ_f due to the fact that the design formula has been set to pass at the margin (or fringe) of the experimental scatter band width rather than through its middle.

The situation is illustrated in Fig. 1. It shows all the points of the ACI (1962) database containing only small beams (accurately plotted from the table in the original source) and also shows the fit of the histogram of v_c data by a Gaussian distribution. This database still serves as the basis of the current ACI 318-05 shear design provisions. The ACI 318-05 formula for required average shear strength is shown by the horizontal line at $v_c = 2\sqrt{f'_c} = v_c = 2\sqrt{0.7f'_{cr}} \approx 1.67\sqrt{f'_{cr}}$.

The recent Toronto tests of two companion beams 74.41 in. (1.89 m) deep, one with and one without stirrups, are shown by the diamond points. The percentage strength reductions marked in Fig. 1 show that the creators of ACI Formula $2\sqrt{f'_c}$ considered it necessary, from the safety viewpoint, that their formula be set at approximately $\sqrt{0.7} \times 65\%$, that is, 54%, of the mean of their test database (note the separation of the horizontal line $2\sqrt{f'_c}$ and the line $3.1\sqrt{f'_{cr}}$ for the mean of database).

The Toronto test without stirrups represents $0.74/3.1 = 23.8\%$ of the mean of the database, and so the strength reduction due to size effect is, for this test, 23.8%. But what strikes the eye immediately is that not only the point for the beam without stirrups, but also the point for the beam with minimum stirrups, lies far below the mean of the database, precisely at $1.83/3.1 = 59\%$ of the mean. This indicates that the size effect reduced the strength of the Toronto beam with minimum stirrups to 59% of the average strength of the small-beam database—a reduction that is not negligible at all.

The benefit provided by the minimum stirrups in the Toronto tests was that the size effect reduction of V_c was mitigated from 23.8 to 59%. That is helpful, but insufficient for safety by far. Even with stirrups, the failure probability is several orders of magnitude higher than one in 1 million.

The aforementioned two covert understrength factors implied by the current ACI 318-05 code provisions are 65 and 83.7%, as shown in Fig. 1. If these factors were unnecessary, then the design formula would be $v_c = 2\sqrt{f'_c}/(0.65 \times \sqrt{0.7}) = 3.68\sqrt{f'_c}$ instead of $v_c = 2\sqrt{f'_c}$, but this would, of course, be

unsafe. Obviously, the same safety margin must be satisfied by any subsequent tests, such as the Toronto test.

These observations make it clear that stirrups do not eliminate the size effect. They only mitigate it. According to the theory,⁴² the general size effect Formula (1) remains valid and the effect of stirrups is to increase the transitional size d_0 . Avoidance of size effect would require elimination of post-peak softening on the load-deflection diagram, and this could be achieved only if the concrete were subjected to strong triaxial confinement (all the three negative principal stresses would have to exceed several times the uniaxial compression strength in magnitude⁴³).

The crack band finite element model has been used at Northwestern University to check whether the shear failure of beams with minimum stirrups exhibits a size effect. The beam geometry is the same as in the Toronto tests,^{10,11} except that the longitudinal steel ratio is slightly raised to 1%, to make sure that the beam would not fail by flexure. Computations are run for geometrically similar beams of depths 37.2 in. (0.945 m), 74.4 in. (1.89 m, the size tested in Toronto), and 148.8 in. (3.78 m). The fracture energy of the Toronto concrete is estimated from the empirical formula⁴⁴ as $G_f = 60 \text{ J/m}^2$. The stirrups and longitudinal bars are assumed not to slip.

The mesh and the cracking pattern at maximum load are seen in Fig. 8(a), which shows the simulated dimensionless load-deflection diagrams for all the sizes. The diagram for $d = 74.4 \text{ in.}$ (1.89 m, the size tested in Toronto) shows the peak load of 340 kips (1513 kN), which is close to the measured value (despite a small increase of longitudinal steel ratio). Figure 8(c) shows the dependence of the average beam shear strength $v_n = V/b_w d$ on beam depth d , and Fig. 8(d) shows the same for the average shear strength $v_c = V_c/b_w d$ contributed by concrete ($V_c = V - V_s$, $V_s = A_s f_y d/s$ where A_s and s equal the stirrup area and spacing). These plots document the existence of a strong size effect. The asymptotic slope $-1/2$ of the size effect is also shown.

To explore the effect of longitudinal steel ratio ρ_w , the crack band finite element calculations are also run for increasing ρ_w values (and for fixed size $d = 74.4 \text{ in.}$ [1.89 m]) (refer to Fig. 8(b)). It transpires that an increase of ρ_w raises the shear capacity V of these beams, but only up to a certain critical value, $\rho_w \approx 0.9\%$. For a further increase in ρ_w (and up to 75% of the balanced steel ratio ρ_b), the shear capacity slightly decreases and then levels off.

The conclusion from these finite element simulations is that the shear reinforcement, whether minimum or heavier than minimum, is unable to suppress the size effect. It mitigates the size effect significantly, but not enough by far to make the size effect negligible.

CLOSING COMMENTS

At present, the concrete design experts are not yet in complete agreement. As pointed out, several alternative formulas for size effect, including those of JSCE, CEB-FIP, and ACI Subcommittee 445F, are being debated. They do not show major differences within the range of the existing database but give very different extrapolations to very large beams. The extrapolation according to Eq. (2) gives much smaller V_c values than the other formulas for beam depths of the order of 393.7 in. (10 m). Even if the present rational arguments are set aside, the prudent choice is the formula offering the safest extrapolation of the database to large sizes, which is Formula (2). If calibrated to the same database, this

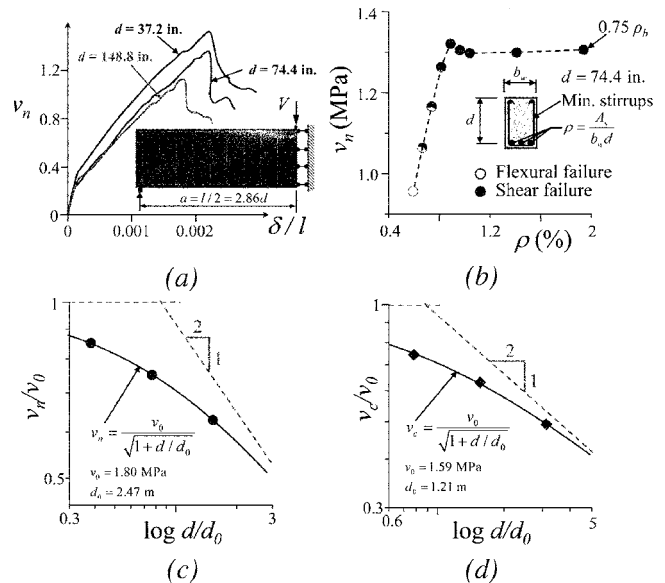


Fig. 8—Crack band finite element simulations for shear failure of beams with stirrups.

formula will always give, for sizes beyond the database range, lower values of V_c than the JSCE, CEB-FIP, and ACI Subcommittee 445F formulas.

In view of costs, real-size tests of extremely large beams are hardly feasible, and even moderately large beams cannot be tested in sufficient numbers (and for a sufficient range of shear spans, steel ratios, and concrete types), so as to provide statistically significant evidence for an empirical formulation. Some information, however, can be extracted from past structural disasters. Their recent studies show that the size effect must have been a contributing factor in many of them. The reason that this was not initially recognized is that the true overall safety factor (the ratio of the mean of test results to the unfactored design service load) is huge—approximately 3.5 to 7 for shear failures of the small laboratory-size beams,⁴¹ and, even after taking the size effect into account, still approximately 1.7 to 3.5 for the largest.

Therefore, not one mistake, but typically two or more mistakes, are usually needed to cause shear failure of a reinforced concrete beam. Unfortunately, multiple mistakes can happen, and doubtless will. When they do, designing for size effect can make the difference between failure and survival.

ACKNOWLEDGMENTS

The work of the first two authors was supported by the Department of Transportation through the Infrastructure Institute of Northwestern University, under Grant No. 0740-357-A475.

REFERENCES

1. Joint ACI-ASCE Committee 326, "Shear and Diagonal Tension," *ACI JOURNAL, Proceedings* V. 59, No. 1-3, Jan.-Mar. 1962, pp. 1-30, 277-344, 352-396.
2. Bažant, Z. P., and Kim, J.-K., "Size Effect in Shear Failure of Longitudinally Reinforced Beams," *ACI JOURNAL, Proceedings* V. 81, No. 5, Sept.-Oct. 1984, pp. 456-468; discussion and closure, V. 82, No. 4, July-Aug. 1985, pp. 579-583.
3. Bažant, Z. P., and Sun, H.-H., "Size Effect in Diagonal Shear Failure: Influence of Aggregate Size and Stirrups," *ACI Materials Journal*, V. 84, No. 4, July-Aug. 1987, pp. 259-272.
4. Bažant, Z. P., and Kazemi, M. T., "Size Effect on Diagonal Shear Failure of Beams without Stirrups," *ACI Structural Journal*, V. 88, No. 3, May-June 1991, pp. 268-276.
5. Iguro, M.; Shioya, T.; Nojiri, Y.; and Akiyama, H., "Experimental Studies on Shear Strength of Large Reinforced Concrete Beams under

Uniformly Distributed Load,” *Concrete Library International of JSCE*, No. 5, 1985, pp. 137-146.

6. Shioya, T.; Iguro, M.; Nojiri, Y.; Akiyama, H.; and Okada, T., “Shear Strength of Large Reinforced Concrete Beams,” *Fracture Mechanics: Application to Concrete*, SP-118, V. C. Li and Z. P. Bažant, eds., American Concrete Institute, Farmington Hills, Mich., 1989, pp. 259-279.

7. Shioya, T., and Akiyama, H., “Application to Design of Size Effect in Reinforced Concrete Structures,” *Size Effect in Concrete Structures, Proceedings of the Japan Concrete Institute International Workshop*, H. Mihashi, H. Okamura, and Z. P. Bažant, eds., E&FN Spon, London, UK, 1994, pp. 409-416.

8. Kani, G. N. J., “How Safe are Our Large Reinforced Concrete Beams?” *ACI JOURNAL*, *Proceedings* V. 64, No. 3, Mar. 1967, pp. 128-141.

9. Podgorniak-Stanik, B. A., “The Influence of Concrete Strength, Distribution of Longitudinal Reinforcement, Amount of Transverse Reinforcement and Member Size on Shear Strength of Reinforced Concrete Members,” MASC thesis, Department of Civil Engineering, University of Toronto, Toronto, Ontario, Canada, 1998, 771 pp.

10. Angelakos, D.; Bentz, E. C.; and Collins, M. P., “Effect of Concrete Strength and Minimum Stirrups on Shear Strength of Large Members,” *ACI Structural Journal*, V. 98, No. 3, May-June 2001, pp. 290-300.

11. Lubell, A.; Sherwood, T.; Bentz, E.; and Collins, M. P., “Safe Shear Design of Large, Wide Beams,” *Concrete International*, V. 26, No. 1, Jan. 2004, pp. 67-78; and Letter to the Editor by Bažant and Yu.

12. ACI Committee 446, “Proposal for ACI 318 Code Update for Size Effect of Beam Depth in Shear Design of Reinforced Concrete Beams without Shear Reinforcement,” *Structural Engineering*, Report 0508/A210a, Department of Civil Engineering, Northwestern University, Evanston, Ill., 5 pp.

13. Bažant, Z. P., and Yu, Q., “Designing Against Size Effect on Shear Strength of Reinforced Concrete Beams without Stirrups: I—Formulation,” *Journal of Structural Engineering*, ASCE, V. 131, No. 12, 2005, pp. 1877-1885.

14. Bažant, Z. P., and Yu, Q., “Designing Against Size Effect on Shear Strength of Reinforced Concrete Beams without Stirrups: II—Verification and Calibration,” *Journal of Structural Engineering*, ASCE, V. 131, No. 12, 2005, pp. 1886-1897.

15. Duckett, W., “Risk Analysis and the Acceptable Probability of Failure,” *The Structural Engineer*, Aug. 2005, pp. 25-26.

16. Nordic Committee for Building Structures, “Recommendation for Loading and Safety Regulations for Structural Design,” *NKB Report*, No. 36, 1978.

17. Melchers, R. E., *Structural Reliability Analysis and Prediction*, Wiley, New York, 1987, 456 pp.

18. Reineck, K.-H.; Kuchma, D. A.; Kim, K. S.; and Marx, S., “Shear Database for Reinforced Concrete Members without Shear Reinforcement,” *ACI Structural Journal*, V. 100, No. 2, Mar.-Apr. 2003, pp. 240-249.

19. Bažant, Z. P., and Yu, Q., Letter to the Editor on “Safe Design of Large Wide Beams,” by A. Lubell, T. Sherwood, E. Bentz, and M. Collins, *Concrete International*, V. 28, No. 8, Aug. 2004, pp. 14-16, and rebuttal, pp. 16-17.

20. Yu, Q., discussion of “Shear Database for Reinforced Concrete Members without Shear Reinforcement,” by K.-H. Reineck, D. A. Kuchma, K. S. Kim, and S. Marx, *ACI Structural Journal*, V. 101, No. 2, Jan.-Feb. 2004, pp. 141-143.

21. Bažant, Z. P., and Kazemi, M. T., discussion of “Repeating a Classic Set of Experiments on Size Effect in Shear of Members without Stirrups,” by E. C. Bentz and S. Buckley, *ACI Structural Journal*, V. 103, No. 5, Sept.-Oct. 2006, pp. 754-756.

22. Yu, Q., and Bažant, Z. P., discussion of “Repeating a Classic Set of Experiments on Size Effect in Shear of Members without Stirrups,” by E. C. Bentz and S. Buckley, *ACI Structural Journal*, V. 103, No. 5, Sept.-Oct. 2006, pp. 756-757.

23. Kazemi, M. T., and Broujerdian, V., discussion of “Repeating a Classic Test of Experiments on Size Effect in Shear of Members without Stirrups,” by E. C. Bentz and S. Buckley, *ACI Structural Journal*, V. 103, No. 5, Sept.-Oct. 2006, pp. 757-758.

24. Bažant, Z. P., and Planas, J., *Fracture and Size Effect in Concrete and Other Quasibrittle Materials*, CRC Press, Boca Raton, Fla., 1998, 22 pp.

25. Bažant, Z. P., “Size Effect in Blunt Fracture: Concrete, Rock, Metal,” *Journal of Engineering Mechanics*, ASCE, V. 110, 1984, pp. 518-535.

26. Leonhardt, F., and Walther, R., “Beiträge zur Behandlung der Schubprobleme in Stahlbetonbau,” *Beton-und Stahlbetonbau*, Berlin, Germany, Mar. 1962, pp. 141-149.

27. Bhal, N. S., “Über den Einfluss der Balkenhöhe auf Schubtragfähigkeit von Einfeldrigen Stalbetonbalken mit und ohne Schubbewehrung,” dissertation, Universität Stuttgart, Stuttgart, Germany, 1968.

28. Okamura, H., and Higai, T., “Proposed Design Equation for Shear Strength of Reinforced Concrete Beams without Web Reinforcement,”

Proceedings of the Japanese Society of Civil Engineers, V. 300, 1980, pp. 131-141.

29. Bažant, Z. P., “Scaling Theory for Quasibrittle Structural Failure,” *Proceedings of the National Academy of Sciences*, V. 101, No. 37, 2004, pp. 13,397-13,399.

30. Bažant, Z. P., and Pang, S.-D., “Mechanics Based Statistics of Failure Risk of Quasibrittle Structures and Size Effect on Safety Factors,” *Proceedings of the National Academy of Sciences*, V. 103, No. 25, 2006, pp. 9434-9439.

31. Bažant, Z. P., *Scaling of Structural Strength*, Hermes Penton Science, London, UK, 2004, 280 pp.

32. RILEM Committee QFS, Quasibrittle Fracture Scaling, “State-of-the-Art Report on Quasibrittle Fracture Scaling and Size Effect,” *Materials and Structures*, V. 37, 2004, pp. 547-568.

33. Bažant, Z. P., and Novák, D., 2000, “Probabilistic Nonlocal Theory for Quasibrittle Fracture Initiation and Size Effect: II—Application,” *Journal of Engineering Mechanics*, ASCE, V. 126, No. 2, pp. 75-185.

34. Collins, M. P., and Mitchell, D., *Prestressed Concrete Structures*, Prentice Hall, Englewood Cliffs, N. J., 1991, 720 pp.

35. Bažant, Z. P., and Cedolin, L., *Stability of Structures: Elastic, Inelastic, Fracture and Damage Theories*, 2nd Edition, Dover Publications, New York, 2003, 1056 pp.

36. Ang, A. H.-S., and Tang, W. H., *Probability Concepts in Engineering Planning and Design*, V. 1, Chapter 7, Wiley, New York, 1976, 424 pp.

37. Bažant, Z. P., and Yu, Q., “Minimizing Statistical Bias in Evaluating Database for Size Effect in Beam Shear,” *Infrastructure Technology Institute Report No. 06-07-C605u*, Northwestern University, Evanston, Ill., 2006.

38. Bažant, Z. P., and Yu, Q., “Does Strength Test Exceeding Code Prediction of Nominal Strength Justify Ignoring Size Effect in Shear?” *Infrastructure Technology Institute Report No. 06-07-C605v*, Northwestern University, Evanston, Ill., 2006.

39. Madsen, H. O.; Krenk, S.; and Lind, N. C., *Methods of Structural Safety*, Prentice Hall, Englewood Cliffs, N. J., 1986, 416 pp.

40. Haldar, A., and Mahadevan, S., *Probability, Reliability and Statistical Methods in Engineering Design*, Wiley, New York, 1999, 320 pp.

41. Bažant, Z. P., and Yu, Q., “Reliability, Brittleness, Covert Understrength Factors, and Fringe Formulas in Concrete Design Codes,” *Journal of Structural Engineering*, ASCE, V. 132, No. 1, 2006, pp. 3-12.

42. Bažant, Z. P., “Fracturing Truss Model: Size Effect in Shear Failure of Reinforced Concrete,” *Journal of Engineering Mechanics*, ASCE, V. 123, No. 12, 1997, pp. 1276-1288.

43. Caner, F. C., and Bažant, Z. P., “Lateral Confinement Needed to Suppress Softening of Concrete in Compression,” *Journal of Engineering Mechanics*, ASCE, V. 128, No. 12, 2002, pp. 1304-1313.

44. Bažant, Z. P., and Becq-Giraudon, E., “Statistical Prediction of Fracture Parameters of Concrete and Implications for Choice of Testing Standard,” *Cement and Concrete Research*, V. 32, No. 4, 2002, pp. 529-556.

APPENDIX—DISCUSSION OF DESIGN SITUATIONS NOT COVERED BY EXISTING DATABASE

Beams with low longitudinal steel ratio ρ_w in Joint ACI-ASCE Committee 445 database

Low ρ_w was one point on which concern has been voiced. In the ESDB, ρ_w ranges from 0.14 to 6.64%, with a mean value at 2.3%, and among the 398 tests, only 58 had $\rho_w < 1\%$. Therefore the data for $\rho_w < 1\%$ are plotted separately in Fig. A(a) (in this and further figures with varying ρ_w , the size of each circle is proportional to ρ_w). As can be seen, the fit is just as good as that for the total ESDB, and so there is no problem in this regard.

To clarify the role of ρ_w further, 18 beams, with ρ_w ranging from 0.25 to 8%, have been simulated by a crack-band finite element code with the microplane model (refer to Fig. A(b)). In the computations, all the beams failed by shear. Again, the ACI Committee 446 formula is seen to give a good and safe estimate of shear strength for all the computer-generated data.

Design example: Fixed-end beam under distributed load

The ESDB is restricted to simply supported beams under three- or four-point loading. The proposed code revision, however, will, in practice, be applied also to redundant beams and distributed loading. Although the existing code specifications have, for a long time, been extended the same

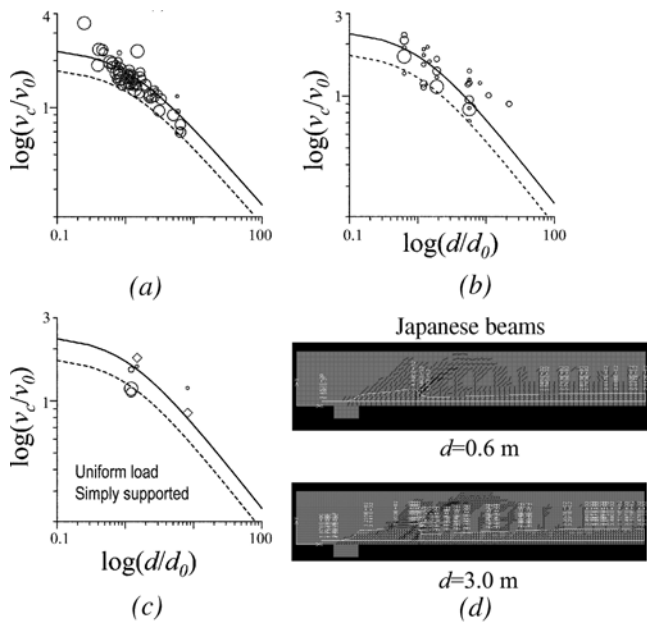


Fig. A—Test and simulations compared with proposed formula: (a) ESDB data with $\rho_w < 1\%$; (b) simulations of beams with different ρ_w ; (c) Japanese tests of simply supported beams under distributed loads and their simulations; and (d) crack patterns for Japanese beams at maximum load.

way, it is proper to check some cases. One case of concern is an example of wide beam (slab) design presented in 2004 at the ACI Committee 446 meeting in Washington, D.C., which seemed to cast doubt on the present proposal. A fixed-end beam with a span of 20 ft (6.1 m), under an 11 ft (3.35 m) overburden of soil, was considered and it was found that the beam depth of $d = 14$ in. (356 mm) with $\rho_w = 1.14\%$ is required according to the current ACI code, and the depth of $d = 34$ in. (864 mm) with $\rho_w = 0.13\%$ would apparently be required by the present code proposal. Due to negative bending moment at ends, this is a case for which no test data exist. Therefore, extensive simulations have been undertaken using a crack-band finite element code to clarify the perplexing conclusion (note that regular commercial finite element codes lacking a nonlocal or crack-band concept cannot be used because they cannot capture the size effect, as a matter of principle).

The simulations of this loading, which is not covered by the current ESDB, include two classical Japanese tests of two beams 23.62 and 118.11 in. (0.6 and 3.0 m) deep,⁷ and further three beams, all of them 14 in. (0.36 m) deep, with $\rho_w = 1, 2,$ and 3% . The results are shown by circles in Fig. A(c), where the two Japanese tests are displayed as diamonds. The simulations agree well with the Japanese tests, and also with the proposed formula. The agreement with the Japanese tests verifies the correctness of the finite element simulation and confirms that the size effect is reproduced. Figure A(d) further documents that the crack patterns at maximum load simulated for the Japanese beams are quite realistic. Figure A(d) also shows the simulated stress distribution along the longitudinal steel bar, in which it should be noted that the longitudinal steel bar does not yield at failure. For the distributed load, the shear span is defined as $a = M/V$, and it needs to be noted that it exceeds 2.5 for all the beams considered herein. This means that these beams fit within the range of validity of the current and proposed ACI specifications.

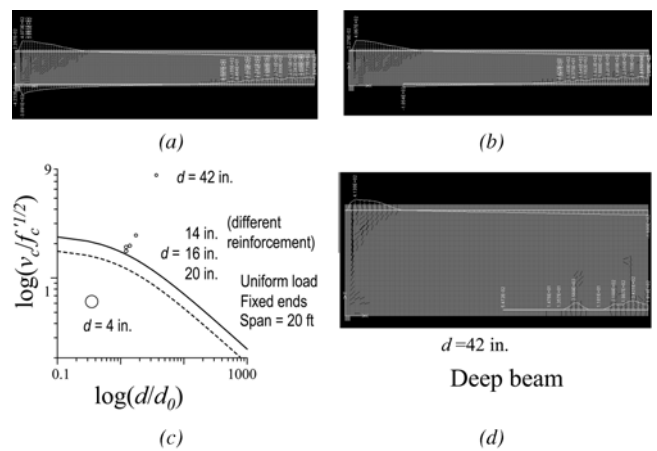


Fig. B—Finite element simulations for Bentz's slab: (a) 14 in. (356 mm) deep slab with steel bar at bottom face across whole span; (b) 14 in. (356 mm) deep slab with steel bar at bottom face terminated 1.5d away from support; (c) simulations of fixed-end wide beams of different thicknesses, of sizes within and outside the range of proposed formula; and (d) 42 in. (1.07 m) deep slab showing deep beam behavior.

The proposed calculation suggested that an incredibly deep beam with incredibly low ρ_w might be required if the present code formula is used. Test data for this situation are lacking. Because of negative bending moment at beam ends, the effect of longitudinal steel entering the compression zone needs to be simulated. Two beams shown in Fig. B(a) and (b) were considered, both with $d = 14$ in. (356 mm), $l = 240$ in. (6.1 m), and $a/d = M/Vd = 2.86$. In the beam on the left, the longitudinal bars at the bottom face run through the whole span, and in the beam on the right, the longitudinal bars terminate at distance $1.5d$ from the supports. All the simulated beams fail by shear (that is, the longitudinal steel does not yield) and exhibit a clear diagonal shear crack at peak load. The beam on the left of the figure has a shear strength higher by 9% than the beam on the right. This result confirms that the shear strength prediction is conservative when there is steel bar in the compression zone. This is not surprising because all finite element simulations show that the shear strength is controlled by compression failure of the concrete above the tip of the diagonal shear crack caused by compression force parallel to the crack.

Although the design strength for both simulations is close to the present proposal (Fig. B(c)), this proposal gives, for $d = 14$ in. (356 mm), a design strength slightly less than the factored load. This is what motivated the proposal to Joint ACI-ASCE Committee 445 to calculate how much the beam depths need to be enlarged to satisfy the present code proposal. The calculation indicated that $d = 34$ in. (864 mm) was needed if the present proposal were used. It was overlooked in this calculation, however, that the present code proposal, as well as the current code, becomes invalid once d exceeds 16 in. (406 mm). The reason is that the beam becomes a deep beam, which is defined as a beam with $a/d \leq 2$ and requires a different design procedure, based on the strut-and-tie model. Using this procedure, one finds that the necessary depth in the proposed example is $d = 20$ in. (508 mm), and not 34 in. (864 mm).

This conclusion cannot be checked by the ESDB because of its limitation to beams with $a/d \geq 2.5$. Therefore, for

further clarification, four other beams are simulated by a computer program. All parameters are the same except that $d = 4, 16, 20,$ and 42 in. (100, 406, 508, and 1067 mm) at constant beam span $L = 20$ ft (6.1 m). The ratio a/d decreases with increasing d , and this is seen to increase the shear strength rapidly. The crack propagation and stress distribution along the steel bar in the beam of 42 in. (1067 mm) depth are plotted in Fig. B(d). A typical short beam failure is clearly seen, and the steel bar yields at peak load. Formula (2) gives good predictions for $d = 14, 16,$ and 20 in. (356, 406, and 508 mm) even though it is supposed to apply only for $d \leq 16$ in. (406 mm) (which corresponds to $a/d \geq 2.5$). For unusually

small depths, however, $d < 4$ in. (100 mm, $a/d > 10$), the simulated shear strength is much less than predicted, which suggests that an upper bound, $a/d \approx 8$, might be considered for adoption, with a different formula for higher a/d . The reason is that, in very slender beams, the region having, at maximum load, very high compressive stress (close to f'_c) is found to be much more elongated than for normal a/d , and this apparently promotes crushing of concrete. Such inferences cannot be checked with the ESDB, however, in which the maximum a/d is 8.03. To cover a large a/d , which is not included in the ESDB, the parameter a/d will have to be included in Eq. (2).

Disc. 104-S51/From the September-October 2007 *ACI Structural Journal*, p. 542

Thermal Movements in Parking Structures. Paper by Mohammad Iqbal

Discussion by Gary Klein and Richard Lindenberg

ACI member, Wiss, Janney, Elstner Associates, Inc., Northbrook, IL; Davis Bowan & Friedel, Salisbury, MD

This paper discusses a very important but frequently misunderstood aspect of parking structure design. The paper provides very interesting data on actual movements of post-tensioned and precast parking structures. The discussers are the principal investigators for an ongoing PCI-funded study on volume change effects in precast buildings, which is referred to by the author.

Under the discussion of thermal coefficient of expansion, the author contends that PCI reduces the temperature strains by a factor of 1.5 when computing thermal shortening. Although the *PCI Handbook*⁵ is not as clear as it perhaps should be, it does not recommend using the 1.5 factor for reducing thermal shortening; rather, the factor is used to estimate equivalent volume change strains for purposes of calculating volume change forces. As indicated in Section 3.4.3.1 of the handbook, "...since the shortening takes place gradually over a period of time, the effect of the shortening on the shears and moment of the support is lessened because of creep and micro cracking of the member and its support." In other words, the 1.5 factor is solely for the purpose of calculating member forces based on *equivalent* shortening. Appropriately, the design examples in the handbook do not use the 1.5 factor for calculating temperature shortening.

The author correctly points out that the *PCI Handbook*⁵ recommends a 25% reduction in computed thermal strains due to the thermal lag effect. The author argues that thermal lag effects are very small and should be conservatively ignored when the computing volume change movement. Referring to the PCI study that the discussers are now completing, the author notes that summer temperatures outside parking structures are on the order of 10 °F (5.6 °C) hotter than ambient temperatures inside the parking structure. Because thermal shortening is even more critical than thermal expansion, it should have also been noted that ambient temperatures inside parking structures are somewhat warmer than the outdoor temperatures in winter months, especially in the lower levels. As a result of these temperature differences, the thermal response of parking structures is less extreme than would be predicted based on ambient temperatures. In other words, the thermal lag effect is primarily due to the less extreme microclimate inside the structure. The discussers agree with the author that the lag associated with the time it takes for a structural element to reach ambient temperature is indeed not very significant. Nonetheless, some reduction in thermal strains calculated based on extreme outdoor temperatures is appropriate. A reduction of 25% approximates the combined microclimate and thermal lag effects at the lowest level of parking structures, where volume change forces are most significant. The reduction at the upper levels is much less and, as suggested by the author, may be conservatively neglected.

Referring to Fig. 9 of the paper, it is interesting to note the extreme scatter of observed thermal movements in precast

parking structures. Based on the data, the author recommends a movement factor of 0.6 for precast parking structures (compared with 0.8 for post-tensioned parking structures); that is, the author recommends calculating thermal shortening as 60% of the theoretical temperature strain times the length contributing to movement. Given the extreme scatter of the data, higher or lower movement factors are equally justified. The author further recommends a coefficient of thermal expansion of 7.5 microstrains per degree Fahrenheit, which is somewhat higher than the value of 6 microstrains per degree Fahrenheit used in the *PCI Handbook*⁵ and other references. Interestingly, taken together, the author's recommendations result in a calculated thermal shortening for precast concrete structures that is identical to that computed using the current handbook, which includes PCI's 25% reduction for thermal lag. The author's approach is an improvement in the sense that it acknowledges the effect of incremental movements at precast connections in reducing the movement demand at expansion joints. Both the *PCI Handbook*⁵ and author's method provide a reasonable estimate of thermal movement for expansion joint design. As confirmed by the author's observations, actual movement will vary greatly. The paper's documentation of this variability is a significant contribution toward a better understanding of the nature of volume change movement. Managing volume change forces, however, is a problem of even greater complexity and variability. Designers must accommodate both movements and forces without damaging the structure. The report on the PCI research, due summer of 2008, will highlight the importance of flexible connections and ductile members in managing volume change forces and precluding damage due to volume change movement.

AUTHOR'S CLOSURE

The author appreciates the discussers' interest in the paper. The paper provides an empirical underpinning for the design of expansion joints and proposes an equation (Eq. (1) of the paper) to estimate expansion joint thermal movements. The discussion focuses on two design factors in Eq. (1), namely, design temperature and the movement factor (or *M*-factor). Since the publication of this paper, the author has carried out further investigation on expansion joint design. Both factors will become clearer after the author's subsequent paper on expansion joints is published. Regarding the value of design temperature, the author recommends using the temperature values recommended by the Federal Construction Commission and reproduced by ACI 224.3R-95.¹² Any further reduction in design temperature values would result in an overstress of expansion joint assemblies, as shown in Fig. 3.

The discussers point to the obvious scatter in the test data to compute the *M*-factors. As stated in the paper, the data includes all readings recorded using constructed parking facilities in service, and not on laboratory samples tested in

a control environment. The lateral-force-resisting systems (LFRS) in the facilities had beam-column frames of various story heights, member sizes, and concrete strengths. These properties affected the LFRS stiffnesses and the restraint to thermal movement to a varying degree. As defined in the paper, the movement factor M is the ratio of actual movement and the calculated unrestrained movement under volume changes. The M -factor indicates a structure's intrinsic capability to move under volume changes, and as such it serves as an index. The M -factor values range from 0 and 1. Under an ideal condition in which a diaphragm is free to move under volume changes, its M -factor will be unity. On the other hand, a diaphragm that is fully restrained by a rigid LFRS extending the full length of the diaphragm has an M -factor of zero. The pretopped precast structures data (Fig. 9) exhibited more scatter than post-tensioned structures' data (Fig. 8) due to the presence of precast joints in the precast construction. The M -factors were computed to represent the upper bound of the movements.

For post-tensioned and field-topped precast parking structures, the M -factor serves a useful index in quantifying

and predicting volume change cracking in a structure. An M -factor of 0.8 means that a structure moves 80% of the total unrestrained movement with the remaining 20% movement consumed in the structural restraint. The 80% movement level also indicates the degree of restraint post-tensioned structures may tolerate while performing reasonably well. Therefore, the M -factor helps predict whether a facility would perform well under volume change effects. If a structure's LFRS is designed with an M -factor of 0.8 and higher, it would exhibit minimal volume change cracks. If the LFRS is stiffer and has a lower M -factor, however—say 0.7—the facility is likely to exhibit more volume change cracking. An extremely stiff structure having an M -factor of zero or near-zero would be the most prone to volume change cracking.

A correction to the paper is also cited by the author—on p. 546, third line from the bottom of the right-hand column, the number in the parenthesis is inadvertently noted as 4.8 m. It should be corrected to read 2.4 m.

REFERENCES

12. ACI Committee 224, "Joints in Concrete Construction (ACI 224.3R-95)," American Concrete Institute, Farmington Hills, MI, 1995, 42 pp.

Disc. 104-S52/From the September-October 2007 *ACI Structural Journal*, p. 549

Test of High-Rise Core Wall: Effective Stiffness for Seismic Analysis. Paper by Perry Adebar, Ahmed M. M. Ibrahim, and Michael Bryson

Discussion by Himat Solanki

Professional Engineer, Building Dept., Sarasota County Government, Sarasota, FL

The authors have presented an interesting concept on the effective stiffness of core/structural walls. The discussor would like to offer the following comments:

1. The authors have proposed Eq. (3) based on a limited test series of walls having an h_w/l_w ratio equal to or greater than 3.0. Also, walls in the references studied by the authors were rectangular, except for References 9 and 12, which cover walls having end boundary elements and T-shaped walls. It was very difficult to determine the effective stiffness of a wall with a T-shape due to the loading patterns. Also, three walls in Reference 11 have a staggered opening, which further complicates the analysis. There are few references¹⁸⁻²¹ that address the wall h_w/l_w ratio of 3.0 or higher.

2. In Reference 22, the following equation is suggested for structural walls

$$I_e = \left[\frac{14.5}{f_y} + \frac{P_u}{f'_c A_g} \right] I_g \quad (5)$$

It can be seen that authors' Eq. (3) is inconsistent with Eq. (5).

3. If structural walls are considered as a wall-column concept,²³ the I_e can be considered as outlined in Reference 24 and can be presented as follows

Effective moment of inertia I_e

	Range	Recommended value
$P/f'_c A_g \geq 0.5$	$0.70I_g$ to $0.90I_g$	$0.80I_g$
$P/f'_c A_g = 0.2$	$0.50I_g$ to $0.70I_g$	$0.60I_g$
$P/f'_c A_g = -0.05$	$0.30I_g$ to $0.50I_g$	$0.40I_g$

Based on References 23 and 24, the authors' Eq. (3) is again inconsistent with the aforementioned values because, for example, when $P/f'_c A_g = 0.5$, the authors' I_e will be I_g instead of $0.80I_g$ or $0.90I_g$. In addition, when the authors' value of $P/f'_c A_g = -0.05$, the authors' I_e will be $0.55I_g$ instead of $0.40I_g$ or $0.50I_g$.

3. Based on the test series of Reference 20 (high axial load ratio), the I_e becomes equal to I_g , and for a wall tested in Reference 18, the I_e again becomes inconsistent with the test results.

4. The discussor has studied walls having an h_w/l_w ratio equal to or greater than 3.0, as tested in References 1, 4, 7, 9, 12, and 18-21, and the authors presented them in the paper. The following equation was derived by using Reference 22 concepts

$$I_e = \left[\frac{24.5}{f_y} + \frac{P_u}{f'_c A_g} \right] I_g \leq 0.8I_g \quad (6)$$

Equation (6) considers not only the steel stress but also the width of rectangular walls based on the recommended value as specified in ACI 318-05.²⁵

5. Based on the aforementioned studies, the discussor believes that the authors should revisit Eq. (3) and (4) of their paper so that they become consistent with other research and other test data. The authors' proposed Eq. (3) or (4) leads to an overly conservative design for the practicing structural engineer and will not be a cost-effective design, especially for high-rise reinforced concrete buildings.

REFERENCES

18. Riva, P., et al., "Cyclic Behaviour of a Full-Scale RC Structural Wall," Technical Report N-18/2002, Dip. di Ingegneria Civile, Università da Brescia, Via Branze, Brescia, Italy. (in Italian)

19. Lestuzzi, P., et al., "Dynamische Versuche Stahlbetontragwänden auf dem ETH-Erdbebensimulator," *Bericht Nr. 240*, Institut für Baustatik und Konstruktion (IBK), ETH, Zurich, Basel: Birkhäuser Verlag, 1999. (in German)
20. Su, R. K. L., et al., "Seismic Behaviour of Slender Reinforced Concrete Walls under High Axial Load Ratio," *Engineering Structures*, V. 24, 2007, pp. 1957-1965.
21. Carvajal, O., et al., "Muros de Concreto Reforzados con Armadura Mínima," *Buletin Technico*, Universidad Central de Venezuela, Facultad de Ingeniería Año 21, Enero-Diciembre, pp. 72-73. (in Spanish).
22. Priestley, M. J. N., and Hart, G. C., "Design Recommendations for Period of Vibration of Masonry Wall Building," *Research Report SSRP 89/05*,

University of California, San Diego, CA, 1989.

23. Nakazawa, A., et al., "Experimental Study on Shear Behavior of R/C Wall-Columns—Using High-Strength Reinforcement of 13,000 kg/cm² Grade—Parts 1-4," *Summaries of Technical Papers*, Annual Meeting of the Architectural Institute of Japan, Tokyo, 1995-1998, pp. 351-358. (in Japanese)
24. Paulay, T., and Priestley, M. J. N., *Seismic Design of Reinforced Concrete and Masonry Buildings*, John Wiley & Sons, Inc., New York, 1991, 768 pp.
25. ACI Committee 318, "Building Code Requirements for Structural Concrete (ACI 318-05) and Commentary (318R-05)," American Concrete Institute, Farmington Hills, MI, 2005, 430 pp.

Disc. 104-S52/From the September-October 2007 *ACI Structural Journal*, p. 549

Test of High-Rise Core Wall: Effective Stiffness for Seismic Analysis. Paper by Perry Adebar, Ahmed M. M. Ibrahim, and Michael Bryson

Discussion by James M. LaFave and Dawn E. Lehman

ACI member, Associate Professor, Department of Civil and Environmental Engineering, University of Illinois, Urbana, IL; Assistant Professor, Department of Civil and Environmental Engineering, University of Washington, Seattle, WA

Structural walls are a commonly-used seismic-force-resisting system, and reliable models to simulate their response are certainly needed (especially for walls in high-rise structures). This paper provides important information related to this need, and the authors are to be commended for their valuable contribution. Perhaps most important are the results of the scaled model test of a slender concrete structural wall that represents part of the core of a high-rise building. The wall had a height-to-length (h_w/l_w) ratio of more than 7, contained a relatively modest amount of longitudinal reinforcement, and was subjected to a constant axial compression force (from top to bottom) of approximately 10% of its gross axial strength. The lateral loading was applied using an actuator at the otherwise free top end of the nearly 12 m (39 ft) high wall, which had a nominally fixed base.

Given the 1625 mm (64 in.) length of the test wall and its 127 mm (5 in.) web thickness, one might consider this wall model to be at approximately 1/4 of full-scale. It could further be assumed that the lateral load applied at the top of the wall might represent something akin to the resultant of a linearly varying (that is, inverted triangular) lateral-load distribution over the height of a real building (to achieve a reasonably correct proportion of moment and shear at the base of the wall). Under this assumption, the test wall model would represent an actual (full-scale) structural wall approaching 18 m (59 ft) in height, which is something on the order of a 21-story building. Could the authors briefly comment on whether this assessment is reasonable, and also as to whether an acting (gravity) axial load at the base of $0.1f'_c A_g$ is typical for such a wall or was simply selected for testing expedience?

Assuming that the tested wall represents the bottom 14 stories (or so) of a 21-story building, then one can assess the relative values of bending moment, shear, and axial force in the model compared with the theoretical prototype structure. Moving up the model wall from its base, the bending moment drops linearly, whereas the rate of change in an actual building could be less, depending on the building's response to any particular ground motion. Furthermore, whereas the axial compression in the prototype would be expected to drop almost linearly up the wall (due to the decreasing number of stories above), the axial load in the model remains constant throughout, as does the shear force. The result of these differences suggests that flexural wall

cracking would likely extend even higher in the prototype structure's wall than it did in the model test wall. Using the presented experimental data for lateral load at first visible cracking, and also at the end of the test (when cracking extended the equivalent of approximately four stories up the model wall), the discussers were able to estimate the actual flexural cracking strength (that is, modulus of rupture) of the concrete used in the wall to be nearly $0.6\sqrt{f'_c}$ MPa ($8\sqrt{f'_c}$ psi). Using that value, the flexural cracking would have most likely extended upward by one or more additional stories if the axial compression had actually decreased up the height of the wall. Consequently, the existing flexural cracks in the approximate region of the second to fourth floors would have probably been wider, the extent of reinforcement yielding near the base of the wall might have been greater, and residual drifts would have been larger.

The aforementioned discussion can serve as a basis to explain, in part, why the overall experimental load-displacement behavior of the model wall appears to be so similar to that normally associated with post-tensioned concrete walls, such as the hybrid walls described by Kurama²⁶ and the partially prestressed wall tested by Holden et al.²⁷ This has perhaps been amplified by the method of application of the axial compression load in the authors' test (that is, via external bars passing into and centered on the base of the test specimen). This situation can benefit the structural behavior in terms of both stiffness and strength along the entire height of the wall (including minimizing crack formation and crack opening) without the tendency to contribute to any P - Δ effects in the way that actual gravity loads would.

At model wall test drifts of approximately 0.5% or more (beyond the onset of flexural yielding), the discussers further wonder whether there could have been any additional contribution toward system flexibility from shear distortions occurring near the base of the wall. It has previously been noted by Kim et al.²⁸ that, even in reinforced concrete structural walls having relatively low shear stress demands and levels of diagonal cracking, the shear deformations can contribute to the flexibility of the system. This deformation mode is typically triggered after flexural yielding and would physically involve slip along the wider flexure cracks, resulting in behavior even more pinched than for just flexural yielding. From the figures in the paper, it does not appear that

instrumentation to explicitly measure this phenomenon was used in the test, therefore it is difficult to decipher any contribution of such shearing deformations in this test for comparison with other test data.

Finally, the discussers found some of the recommendations for effective stiffness ratio (I_e/I_g) to deviate from their own findings. The second discusser, along with a colleague, has studied the effective stiffness as a function of drift from a variety of experimental structural concrete wall data found in the literature.^{5-6,29-36} The considered tests comprise nearly 35 cases, divided roughly evenly between planar rectangular and barbell wall shapes; nearly half of these tests are the same as some of those summarized in the authors' Table 1. The tests examined by the discussers had wall aspect ratios (h_w/l_w) ranging from 1 to more than 6, with axial compression ratio values ($P/f'_c A_g$) between zero and approximately 0.35. For these cases, I_e/I_g was seldom more than 0.6 for drifts beyond approximately 0.3%, nor more than approximately 0.3 for drifts greater than 0.9%, with the exceptions being a handful of cases where the axial compression ratio was larger than $0.2f'_c A_g$. These trends would tend to indicate somewhat lower effective stiffness values than those presented by the authors in Fig. 12(c) of their paper.

The discussers appreciate the great challenges and compromises that must be made in conducting large-scale laboratory tests and in then applying the results to practice. Therefore, all of the aforementioned comments are made primarily in an attempt to address a concern that structural designers might end up with a bit too optimistic of a view regarding the equivalent flexural stiffness of this sort of a wall in practice, especially if these results are indeed to be used across the full spectrum of stated design applications from push-over analysis to linear dynamic analysis. On the other hand, actual walls could perhaps exhibit somewhat greater energy dissipation than that seen in this test.

REFERENCES

26. Kurama, Y. C., "Hybrid Post-Tensioned Precast Concrete Walls for Use in Seismic Regions," *PCI Journal*, V. 47, No. 5, Sept.-Oct. 2002, pp. 36-59.
27. Holden, T.; Restrepo, J.; and Mander, J. B., "Seismic Performance of Precast Reinforced and Prestressed Concrete Walls," *Journal of Structural Engineering*, ASCE, V. 129, No. 3, Mar. 2003, pp. 286-296.
28. Kim, T.-W.; Foutch, D. A.; and LaFave, J. M., "A Practical Model for Seismic Analysis of Reinforced Concrete Shear Wall Buildings," *Journal of Earthquake Engineering*, V. 9, No. 3, May 2005, pp. 393-417.
29. Lefas, I. D., and Kotsosovos, M. D., "Strength and Deformation Characteristics of Reinforced Concrete Walls under Load Reversals," *ACI Structural Journal*, V. 87, No. 6, Nov.-Dec. 1990, pp. 716-726.
30. Pilakoutas, K.; Elnashai, A. S.; and Ambraseys, N. N., "Earthquake Resistant Design of Reinforced Concrete Structural Walls," *Report No. ESEE 4/91*, Imperial College, London, UK, Apr. 1991.
31. Sittipunt, C.; Wood, S. L.; Lukkunaprasit, P.; and Pattararattanukul, P., "Cyclic Behavior of Reinforced Concrete Structural Walls with Diagonal Web Reinforcement," *ACI Structural Journal*, V. 98, No. 4, July-Aug. 2001, pp. 554-562.
32. Thomsen, J. H., and Wallace, J. W., "Displacement-Based Design of Slender Reinforced Concrete Structural Walls—Experimental Verification," *Journal of Structural Engineering*, ASCE, V. 130, No. 4, Apr. 2004, pp. 618-630.
33. Vallenias, J. M.; Bertero, V. V.; and Popov, E. P., "Hysteretic Behavior of Reinforced Concrete Structural Walls," *Report No. UCB/EERC-79/20*, Earthquake Engineering Research Center, University of California, Berkeley, CA, Aug. 1979, 266 pp.
34. Wang, T. Y.; Bertero, V. V.; and Popov, E. P., "Hysteretic Behavior of Reinforced Concrete Framed Walls," *Report No. UCB/EERC-75-23*, Earthquake Engineering Research Center, University of California, Berkeley, CA, Dec. 1975, 367 pp.
35. Yanez, F. V.; Park, R.; and Paulay, T., "Seismic Behaviour of Walls with Irregular Openings," *Proceedings of the Tenth World Conference on*

Earthquake Engineering, Madrid, July 1992, pp. 3303-3308.

36. Zhang, Y., and Wang, Z., "Seismic Behavior of Reinforced Concrete Shear Walls Subjected to High Axial Loading," *ACI Structural Journal*, V. 97, No. 5, Sept.-Oct. 2000, pp. 739-750.

AUTHOR'S CLOSURE

The authors appreciate the interest in their paper, which had three main parts. First and foremost was the presentation of results from a test on a large-scale model of a concrete shear wall from the core of a high-rise building. The thoughtful questions and comments by discussers LaFave and Lehman regarding the test will be discussed first. The second part of the paper compared the measured wall response with a nonlinear flexural stiffness model¹⁴ for concrete shear walls, and the final part was a summary of work that had previously been done¹⁵ on estimating effective flexural rigidity to account for cracking of concrete shear walls when using linear dynamic analysis. The comments on this topic will be briefly discussed at the end.

The prototype wall was assumed to be 73.2 m (240 ft) high, and to have a height-to-length ratio of 11. The test wall was assumed to be approximately 1/4-scale, but rather than applying a varying lateral load over an 18.3 m (60 ft) high specimen, the resultant lateral point load was applied at approximately 2/3 that height, and the height of the specimen was reduced accordingly. The level of axial compression, $10\% f'_c A_g$, was selected because it is a typical value of axial compression due to gravity loads in high-rise concrete walls.

It is true that the actual shear force and bending moment diagrams in the prototype wall could be different than what was applied in the test and depends on the building's response to any particular ground motion. The bending moment variation associated with a first mode distribution of lateral load is of particular interest as it causes maximum top wall displacements. The bending moment variation from a point load applied at approximately 3/4 of a cantilever wall height and a first mode distribution of lateral load are almost identical from the base of the wall to approximately midheight.

In an actual high-rise wall, bending moments and shear forces vary in a complex way, both over the height of the wall and from one instance to the next. Nonlinear analysis indicates the shear force (bending moment gradient) will reverse direction a number of times while the bending moment at the base of the wall is relatively constant. The objective of the slow cyclic test on a large test specimen was not to try to simulate this complex behavior, which can only be done on a shake table, but to measure the fundamental flexural behavior of a structural concrete wall with minimal contribution from shear deformations. The bending moment-curvature relationship that was measured during the test is that fundamental property. The constant axial compression over the height of the wall was not only easier to apply in the test, but also meant that all bending moment and curvatures measured over the height of the wall were part of the same bending moment-curvature relationship for the wall.

It is certainly reasonable to question whether applying a constant axial compression (rather than a linearly varying axial compression) had a significant influence on the load-displacement behavior of the wall. The authors believe that it did not because the height of wall significantly contributing to wall drifts was small compared with the 18.3 m (60 ft) height over which the axial compression should have been reduced to zero. Due to the maximum lateral load at 2% drift, approximately 15 flexural cracks occurred over a height of 3.6 m (11.8 ft) above the base. Using this information, and assuming a

concrete tensile strength in bending of 4.2 MPa (0.61 ksi), additional flexural cracking would have occurred over a height of 1.0 m (3.4 ft) if the axial compression had reduced linearly from 10% $f'_c A_g$ at the construction joint to zero at 18.3 m (60 ft) above the base. As the flexural cracks had an average spacing of 240 mm (9.5 in.), four additional flexural cracks would have occurred in the wall. In judging whether these additional cracks would have significantly influenced the load-deformation response of the wall, it is important to note that many of the upper flexural cracks in the wall were small under the maximum lateral load (refer to Table 3) and completely closed when the lateral load was reduced slightly. That is, these cracks were closed for most of the load-deformation response of the wall. Most of the deformation of the wall was the result of approximately half the cracks over 2 m (6.6 ft) of the wall height (refer to Fig. 8 and 9). Over this height, the axial compression should have been reduced by only 11%.

LaFave and Lehman are correct that the method of applying axial compression load in the test by external bars attached to the top of the wall and passing through the base of the wall did not model the $P-\Delta$ effect of gravity loads, and provided some artificial increase in stiffness and strength of the wall. The question again is how significant was the error introduced by the simplifications that were necessary to conduct the test in a laboratory. As drifts are small near the base of cantilever walls where axial compression is large, the $P-\Delta$ effect is generally much smaller in cantilever walls compared with frames. The external bars, which passed through large sleeves in the base of the wall, had an overall length of 15 m (50 ft). Throughout most of the test, the bars seemed to pass freely through the base. That is, they did not appear to be touching the sides of the sleeves. Using the overall length of the external bars, the horizontal component of the 1500 kN (342 kip) force in the external bars would be 4.6 kN (1.05 kip) at a top wall displacement of 46 mm (1.8 in.) when significant yielding of the vertical reinforcement occurred. This corresponds to 3.5% of the applied lateral load. Thus, this effect does not appear to have been significant in the elastic range of the wall.

After yielding of the vertical reinforcement, the lateral displacement increased without a significant increase in lateral load. Thus, the percentage increase in lateral load due to the horizontal component of the external bars used to apply axial compression does increase. Also, it is possible that the external bars did contact the sides of the sleeves at very large top wall displacements. At the maximum drift, the maximum lateral load applied to the wall was 18% larger than predicted based on the measured yield strength of the vertical reinforcement; this increase, however, is partly due to strain hardening of vertical reinforcement. As the ultimate strength of the vertical reinforcement was 40% larger than the yield strength, and calculations indicate 30% of the overturning moment was resisted by vertical reinforcement, the maximum strength increase due to strain hardening was 12%. Thus, it appears that the method of applying axial compression in the test increased the wall strength by at least 6% and likely approximately 10% at maximum drift. This error seems acceptable considering how difficult it would have been to better simulate the influence of gravity loads. The most important conclusion from this discussion is that if gravity loads had been exactly simulated, the small strength increase due to strain hardening of vertical reinforcement would have been eliminated by the small strength reduction

due to the $P-\Delta$ effect of gravity loads, and the load-deformation response of the test wall would have been very flat.

An important question is why the load-deformation response of the current test wall was so different than has been observed with other reinforced concrete walls and so similar to what has been observed with post-tensioned concrete walls. The explanation is not in the details of how the test was conducted, but is the result of an important property of the wall—namely, the relative amount of flexural resistance provided by axial compression versus bonded vertical reinforcement. This explains the flat load-deformation response discussed previously, and explains the pinching of hysteresis loops causing reduced energy dissipation. The latter behavior is related to the bending moment at which flexural cracks near the base of the wall close due to the axial compression. An explanation follows.

If there had been no vertical reinforcement in the test wall, preexisting flexural cracks in the wall would open and close (the wall would rock) at an overturning moment equal to approximately $(P/A)S = 857$ kNm (632 kip-ft), which for the critical crack at the construction joint corresponds to a lateral load of 75.6 kN (17.2 kip). Vertical reinforcement in the wall that has yielded in tension resists closing of the cracks and must yield in compression before the flexural cracks will completely close. If the yield force of the vertical tension reinforcement is large in relation to the axial compression force, the flexural cracks will not close until the bending moment reverses and flexural compression is applied to the tension reinforcement. This behavior, which results in significant residual displacements under zero lateral load, has been observed in most previous tests of reinforced concrete structures. In the current test wall, the yield force of all vertical reinforcement in the tension flange and web is equal to 410 kN (93.5 kip), which is only 27% of the applied axial compression force at the base of the wall. As the centroid of this vertical reinforcement is located at 0.4 m (1.3 ft) from the wall centerline, an axial compression force of 410 kN (93.5 kip) applied at the wall centerline and bending moment of 164 kNm (123 kip-ft) is required to yield this reinforcement. Thus, the overturning moment at which flexural cracks are predicted to close in the test wall is $(1 - 0.27) \times 857 - 164 = 462$ kNm (342 kip-ft). For the lowest flexural crack at the construction joint, this corresponds to a lateral load of 41 kN (9.3 kip). As indicated by the change in slope of the unloading curves shown in Fig. 5, the flexural cracks were all closed when the lateral load was less than approximately 40 kN (9 kip). The residual displacements remaining after the flexural cracks closed were primarily due to misalignment of damaged crack surfaces.

LaFave and Lehman question whether there could have been any contribution toward system flexibility from shear deformations. The test was designed to measure flexural response of a concrete shear wall with minimum contribution from shear deformations. As the maximum shear force that was expected to be applied in the test was considerably less than the concrete contribution V_c for a member subjected to an axial compression of 10% $f'_c A_g$, significant diagonal cracking was not expected in the test, and no instrumentation was installed to measure shear deformations. As reported in the paper, a surprising amount of flexure-shear diagonal cracking was observed in the web of the wall considering that the maximum shear stress V/bI_w was only 0.78 MPa (113 psi) and the axial compression stress P/A was 4.9 MPa (710 psi). The deformations at these cracks were carefully observed during

the test (for example, measured crack widths are reported in Table 3). Very little shear displacement of the crack surfaces was observed. Thus it was concluded that the diagonal cracking did not influence the overall response of the wall other than increasing the spread of inelastic curvatures (that is, increasing plastic hinge length).

It is important to note that, when shear deformations contribute to the flexibility of a wall, the flexural stiffness of the wall is actually larger than what one would estimate by ignoring this contribution from shear deformation. Most other wall tests that have been done to date have had significant contributions from shear deformations. Because of the strong influence of shear on the flexural compression stress distribution and, hence, magnitude of flexural tension, it is difficult to completely separate the influence of shear from flexure. It is for this reason that tests on very slender walls, such as the current test wall, should be used for estimating the flexural stiffness of high-rise concrete shear walls.

Effective stiffness for linear dynamic analysis

The final part of the paper was a summary of work that had previously been done by the authors¹⁵ on what effective flexural rigidity should be used in a linear dynamic analysis (such as response spectrum analysis) to account for cracked sections. The approach taken in Reference 15 to arrive at the recommendations summarized in the current paper was to use the results from a fiber model to develop a simple nonlinear flexural model¹⁴ for typical high-rise concrete shear walls. This nonlinear model was verified by comparing predictions with the results of the large-scale test presented in the current paper. The nonlinear flexural model was then used to predict the load-displacement response of many different high-rise walls, and the results of these were used to develop the recommendations for effective stiffness.

A fundamental assumption used in the previous work is that effective stiffness of a nonlinear member is the slope of the elastic portion of an equivalent elastic-plastic load-displacement relationship that has the same area under the curve as the actual nonlinear load-displacement relationship. Other authors have used other ways to determine effective stiffness such as assuming that the effective stiffness is equal to the secant stiffness to some predefined point on the nonlinear load-displacement relationship. Unfortunately, none of the discussers have indicated how they determined effective stiffness.

The first author and his recent students have continued the work on effective flexural stiffness of high-rise concrete shear walls. Rather than use a simple definition of effective stiffness based on the shape of the nonlinear load-deformation

curve, nonlinear dynamic analysis was used to determine the maximum displacement of a variety of concrete walls subjected to a variety of ground motions. The effective stiffness is that which gives the correct estimate of average maximum wall displacement using linear dynamic analysis. The nonlinear load-deformation response of the walls was determined using the experimentally calibrated nonlinear flexural model.¹⁴

The results of this recent work indicates that the effective stiffness ratio (I_e/I_g) of a concrete shear wall is seldom less than 0.5, and for tall walls with long initial fundamental periods, is seldom less than 0.6. In addition to the characteristics of the ground motion, and initial period of the structure, the ratio of maximum elastic force demand to strength of the wall (R factor) is an important parameter that influences effective stiffness. The level of axial compression has much less influence than previously thought. Axial compression does delay the point that the loading curve becomes nonlinear; but as discussed previously, if the flexural resistance of a wall is primarily provided by axial compression in concrete rather than tension in vertical reinforcement, much less energy is dissipated. This increases maximum wall displacements, which reduces effective stiffness. The stress at which the vertical reinforcement yields is not an important parameter.

Discussor Solanki believes the authors should revisit Eq. (3) and (4) because they are inconsistent with the recommendations for effective stiffness that he has summarized. First, the recommendations he has summarized are themselves inconsistent, as Eq. (5) gives a very different result from Eq. (6). Second, the lower-bound effective stiffness given by Eq. (4) is consistent with Eq. (5) at low levels of axial compression, and is consistent with Eq. (6) at high levels of axial compression for a wall, which is no more than approximately 30% $f'_c A_g$. The statement by discussor Solanki that Eq. (3) and (4) lead to overconservative designs that are not cost-effective is nonsensical. The critical issue in the design of high-rise concrete walls is maximum drift demands. Equations (3) and (4) give higher effective stiffnesses than the other recommendations for typical values of axial compression in high-rise concrete walls, which results in lower maximum drift demands for a given structure or less concrete structure for a given maximum drift.

There were two typographical errors in the paper: 1) the column in Table 1 entitled "Axial composition" should be "Axial compression"; and 2) the definition of the parameter a in Eq. (2) given immediately below the equation should be $a = 1.1(I_{cr}/I_g)^{-0.4}$.

Disc. 104-S57/From the September-October 2007 *ACI Structural Journal*, p. 601

Justification of ACI 446 Proposal for Updating ACI Code Provisions for Shear Design of Reinforced Concrete Beams. Paper by Zdenek P. Bazant, Qiang Yu, Walter Gerstle, James Hanson, and J. Woody Ju

Discussion by Evan C. Bentz

ACI member, Associate Professor, University of Toronto, Toronto, ON, Canada

The authors are to be congratulated for writing a comprehensive paper that summarizes the opinions of ACI Committee 446 on fracture mechanics approaches to shear design. First, it must be noted that the discussor agrees that the size effect should be included in the shear design methods of the ACI Code. Whereas the discussor does not

fully agree with the method being proposed, he welcomes the increased attention to the issue that should result from this paper. The discussor has the following questions and comments on the paper:

1. The authors state that it is inappropriate to trust empirical relations for the effect of depth on shear strength. Despite this,

they seem willing to accept empirical relations for the effect of ρ , a/d , f'_c , and all other variables. Is this not inconsistent?

2. The results of the 1991 shear tests of Bažant and Kazemi⁴ are clearly important to the decision to apply a fracture mechanics approach to shear. Is it appropriate, therefore, to neglect to mention the recent 2005 paper⁴⁵ that presents the results of repeat tests that were inconsistent with the original 1991 tests? The authors refer to three of the discussions to this 2005 paper²¹⁻²³ but not the paper itself. It would seem unfair for the readers to be kept in the dark concerning questions about the repeatability of these experimental results.

3. The paper includes an argument that the 1991 Bažant and Kazemi⁴ experiments should be included in the ACI 445-F database used in this paper. For inclusion in this database,¹⁸ member width needed to be at least 2 in. (50 mm). The authors state that the 1991 beams missed this limit by a "mere 4%," as they were 1.90 in. (48 mm) wide. Bažant and Kazemi⁴ reported that their beams were 1.5 in. (38 mm) wide, not 1.90 in. (48 mm) wide, as stated by the authors. Thus, the member width limit for inclusion in the database was missed by over 30%, not 4%. It is disconcerting that a paper by Bažant and colleagues would accidentally base an argument on factual errors about their own experiments.

4. It is stated that there are only 11 size effect series of tests available for comparison with the fracture mechanics method. A recent paper,⁴⁶ however, includes 24 size effect series. Recent work on a larger database⁴⁷ has uncovered additional test series, giving a total of 38 published size effect series on shear strength. The authors may wish to expand their database and see if their conclusions apply to all published size effect tests.

5. The discussor is concerned with the argument being made in relation to Fig. 5. Because the value of d_0 is a statistical curve-fit parameter, the same individual set of experiments could show up as fully consistent with the theory of fracture mechanics whether they showed no size effect, a medium size effect, or a very strong size effect. Once natural experimental scatter is included, it would appear that just about *any* set of experimental points measured with respect to size can be declared fully consistent with the theory of fracture mechanics. This would mean that the theory is non-falsifiable in terms of its application to the shear strength of reinforced concrete beams. To demonstrate that the theory is falsifiable and, therefore, a productive scientific theory, what predictions can the authors make based on the fracture mechanics approach to shear that could be used to test the theory experimentally?

6. Figure 8 shows the results of a fracture mechanics-based finite element (FE) model predicting the shear strength of members with stirrups based on a test from Toronto.¹¹ The discussor is surprised at the predicted shear strength values shown in Fig. 8(b). Scaling off the figure, the theoretically predicted shear stress at shear failure on the top part of the figure is 189 psi (1.30 MPa). Is it a coincidence that the ACI Code also predicts the same shear stress at failure of $2\sqrt{4870 + 50} = 189$ psi (1.30 MPa)? It appears that the finite element results have been curve-fit to match the ACI Code for the particular details of the Toronto test. Should the reader interpret this as a vote of validation for the ACI Code method for members with stirrups? Is not the relatively complex statistical discussion on the page leading up to this figure invalidated by having theoretical FE results in the paper showing that the fracture mechanics approach gives the same answers as the existing ACI Code for members of a large depth with stirrups?

REFERENCES

45. Bentz, E. C., and Buckley, S., "Repeating a Classic Set of Experiments on Size Effect in Shear of Members without Stirrups," *ACI Structural Journal*, V. 102, No. 6, Nov.-Dec. 2005, pp. 832-838.
46. Bentz, E. C., "Empirical Modeling of Reinforced Concrete Shear Strength Shear Size Effect for Members Without Stirrups," *ACI Structural Journal*, V. 102, No. 2, Mar.-Apr. 2005, pp. 232-241.
47. Collins, M. P.; Bentz, E. C.; and Sherwood, E. G., "Where is Shear Reinforcement Required? A Review of Research Results and Design Procedures," *ACI Structural Journal*, V. 105, No. 5, Sept.-Oct. 2008.

AUTHORS' CLOSURE

The authors deeply appreciate the thoughtful and stimulating questions of discussor Bentz, which provide an opportunity to clarify points that were not specifically addressed in the paper. His six points are answered as follows:

1. The reason why empirical relations can be used for the effects of steel ratio ρ_w , relative shear-span ratio a/d , and concrete compressive strength f'_c , but not for the effect of size, is the difference between interpolation and extrapolation. Interpolation of experimental data can provide sufficient accuracy, but extrapolation cannot. Extrapolation can be trusted only if it is based on a good theory that must, of course, be verified by experiments.

The experiments can be of different kinds, for example, reduced scale tests with reduced aggregate size and tests of specimens with different geometries. For ρ_w , a/d , f'_c , and d_a , beam shear tests can, and have been, conducted to cover the entire practical ranges of these variables, sampling them with an almost uniform statistical density of distribution. But for the effect of size, unfortunately, the existing database has an enormous statistical bias for small sizes. The practical range of interest extends from depth $d \approx 50$ mm (19.7 in.) to at least 15 m (or 50 ft). For example, the depth of the girder of the Koror-Babeldaob Bridge in Palau, which collapsed, was 14.2 m (or 46.5 ft). In the ACI 445 database,¹⁸ however, 86% of all the data pertain to $d < 0.5$ m (19.7 in.), 99% to $d < 1.1$ m (43.3 in.), and 100% for $d < 2.0$ m (79 in.).

Therefore, the design for $d > 0.5$ m (19.7 in.) represents predominantly, and for $d > 1$ m (39.4 in.) almost totally, an extrapolation. It is because of the cost of large-scale tests that beams with $d > 3$ m (118.1 in.) have never been tested to failure, and generally for any size $d > 1$ m (39.4 in.), it is next to impossible to conduct failure tests to cover the entire range of ρ_w , a/d , f'_c , and d_a . On the other hand, for small beams, the ACI 445 database does cover the entire range of these influencing variables, and does so with reasonable uniformity. So, the semi-empirical relations for the effect of these four parameters, which are based mainly on the research of Shioya and Akiyama,⁷ Kani,⁸ Reineck et al.,¹⁸ and Pauw,⁴⁸ are adequate and can be trusted. For the effect of size d , empirical formulas could be trusted for $d < 0.5$ m (19.7 in.), which is still interpolation, but not for extension to larger sizes d , which represent extrapolation, yet are of the main interest for practice. A well founded, experimentally verified theory is the only one to trust.

2. There was no intention to "keep the readers in the dark" about the Bentz's 2005 paper.⁴⁵ Although this paper presented very valuable new test results, it was not referenced because, if it were, some extraneous comments would have been necessary. In particular, it would have been necessary to explain why the interpretation of the 1991 tests of Bažant and Kazemi⁴ was misleading, and the length limit of ACI papers did not allow for adding such an explanation. Contrary to what was claimed, the experiments that Bentz reported in that

paper were not a realistic reproduction of the 1991 experiments, as explained in the cited discussion of his paper.

3. As Bentz pointed out, the width of the 1991 test specimen was indeed 38 mm (1.5 in.),⁴ not 48 mm (1.90 in.), and we regret the error. However, Bentz's argument for excluding these tests from the database is nonetheless invalid. It has been well documented that the beam width increase has a negligible effect on the shear strength if it exceeds approximately four aggregate sizes, and the width of the 1991 test specimens was eight aggregate sizes. Therefore, the beams 38 mm (1.5 in.) wide must have given the same results for shear strength v_c as beams 254 mm (10 in.) wide, and thus there was no reason to exclude them from the ACI database. This exclusion has been especially unfortunate for the advocates of fracture mechanics-based theory of size effect on beam shear strength because these reduced-scale tests provide the best experimental support for the applicability of this theory.

4. Bentz claims that 24, rather than 11, size effect test series are available for comparison to the fracture mechanics-based theory.⁴⁶ From careful examination, however, it transpires that his expansion of the size-effect database is mainly due to questionable loosening of the requirement for geometric similarity and questionable narrowing of the requirement for breadth of the size range. The required range is proportional to the scatter band width (in the log-log plot); it must exceed it by a factor of at least 6 (this follows from the requirement that $\omega_{y/x}/\omega_x < 0.15^{49}$). Otherwise, the regression line has a great error.^{49,50} In the size effect tests used in the paper, most of the test series have a size range greater than 1:8, which is barely sufficient to obtain unambiguous results. In the size effect tests collected by Bentz, over half of the test series have a size range close to 1:4, which is statistically insufficient for determining the size effect. The acceptance of data with insufficient size range is what led Bentz to questionable conclusions about the size effect.⁴⁶

5. Regarding Fig. 5, it must be emphasized that d_0 is not a curve-fitting parameter. Based on fracture mechanics, d_0 can be calculated from the dimensionless energy release function $g(\alpha)$ (obtainable from handbooks) and the material characteristic length identified from tests of fracture specimens of different sizes. To calculate function $g(\alpha)$ for shear of a reinforced concrete beam, a complete analysis of propagation of diagonal, flexural, and compressive shear cracks would be needed. This is a difficult problem, not yet solved. It is for this reason that the size effect formulation proposed in the paper could not be based on a theory in its entirety.

Bentz is right that data exhibiting size effects of different slopes in the log-log plot could be matched to the proposed size effect equation just by adjusting d_0 , so that the data would get positioned on the portion of the size effect curve that has the appropriate slope. Such ambiguous, or falsifiable, matching, however, is possible only for test data of limited size range (<1:4). The match becomes unique for data of a broad enough size range for which the transition from a near-zero slope to the slope of $-1/2$ in a log-log size effect plot is clearly visible. Data whose range is broad enough to show the transition from zero slope to slope $-1/2$ cannot be fitted by other proposed size effect equations, including the power law of exponent $-1/3$ (as proposed in ACI 445) or $-1/4$ (according to the JSCE equation). Also, they certainly cannot be fitted by the modified compression field theory, which gives a size effect curve terminating, in the log-log plot, with the slope of -1 (that is, a power law of exponent -1). Such an excessive slope is

theoretically unjustifiable, thermodynamically impossible, and has no experimental support.

6. The discussor is not right in saying that "the finite element results have been curve fit to match the ACI Code," nor is he right in regarding the shear strength values in Fig. 8(b), computed for beams with stirrups by a fracture mechanics-based finite element code, as a "vote of validation of ACI Code method for beams with stirrups." The problem is that he, like most researchers in this field, overlooked the covert safety margin that is hidden in the ACI Code provisions (as discussed in detail in Reference 41), and is not uncovered unless one carefully examines the database used in setting up the code equation. The safety margins separating the ACI Code equation from the experimental database must be the same as those separating the Toronto experiments from those equations (or else that covert safety margin would be unnecessary and could be removed from the ACI Code or, in other words, the factor of 2 in the formula $v_c = 2\sqrt{f'_{cr}}$ could be increased).

The finite element calculations were based on the mean compression strength of concrete (which was reported as $\bar{f}_c = 33.6$ MPa [4870 psi]). The discussor does not take into account that the ACI Code equation $v_c = 2\sqrt{f'_{cr}}$ was not set to match the mean of the database points (as seen in Fig. 1 of the paper). Rather, it was set to lie at the lower margin of this database, representing a 5% probability cutoff (as calculated from a Gaussian distribution of v_c fitted to the database). This cutoff equals 65% of the mean v_c (as marked in Fig. 1 of the paper; for more detail, refer to Fig. 1(a) of Reference 41).

Consequently, the value of $v_c = 0.96$ MPa (140 psi), which Bentz calculated from f'_{cr} according to the ACI Code equation, is not the expected experimental value of v_c (in the sense of the expectation E in statistics). Rather, the expected experimental value is $v_c = 0.96/0.65 = 1.48$ MPa (215 psi), and this value is 1.54 (= $1/0.65$) times higher than the experimental result in the Toronto tests. Thus it must be concluded that the ACI Code equation, when applied to the beams of the size tested in the Toronto tests, overpredicts v_c by 54%.

The value of v_c is, of course, random. Were it possible to test not one but hundreds of beams of the same large depth, with many different concretes, different shear spans, and different longitudinal and stirrup steel ratios, covering the entire ranges of these variables, surely a statistical distribution of v_c with a large standard deviation would be found. To suppose that the Toronto result lies below the 5% cutoff of this undocumented distribution, however, would be dangerous, wishful thinking.

To get a clue where the v_c value from the Toronto large beam test is positioned on this distribution, one would need to carry out, with the same concrete, geometrically similar, reduced-scale tests for depth d between 0.152 and 0.254 m (6 and 10 in.). Within that range, many test results are available to determine the statistical distribution of v_c (which may be assumed to be Gaussian), and many more can be generated at low cost. It may now be checked to which cutoff probability the reduced-scale test corresponds on this distribution (marked in Fig. 4 of Reference 51 by distance a from the mean). It is then logical to assume that the Toronto large beam test would correspond to the same probability cutoff (distance a from the mean) on the distribution of v_c if it could be tested for that size. In this way, the error of the ACI Code equation could be assessed. For beams without stirrups, this was demonstrated in Reference 51. It must be concluded that the ACI Code equation overpredicts the shear stress v_c in the large beam by almost 54%. This is serious indeed. So the calculation

in the paper is not a “vote of validation for the ACI Code method.” Rather, it raises a serious question about the factor of safety of the ACI Code equation when applied to large beams with stirrups. If the size effect is ignored, the safety margins are reduced.

REFERENCES

48. Pauw, A., “Static Modulus of Elasticity of Concrete as Affected by Density,” *ACI JOURNAL, Proceedings* V. 57, No. 12, Dec. 1960, pp. 679-688.

49. Bažant, Z. P., and Pfeiffer, P. A., “Determination of Fracture Energy from Size Effect and Brittleness Number,” *ACI Materials Journal*, V. 84, No. 6, Nov.-Dec. 1987, pp. 463-480.

50. Bažant, Z. P., and Planas, J., *Fracture and Size Effect in Concrete and Other Quasibrittle Materials*, CRC Press, Boca Raton, FL, (textbook and reference volume, 616 + xxii pp.).

51. Bažant, Z. P., and Yu, Q., “Consequences of Ignoring or Misjudging the Size Effect in Concrete Design Codes and Practice,” *Concrete Technology* (Taiwan), V. 1, No.1, 2007, pp. 29-55 (authorized republication, with updates, from *Proceedings of the 3rd Structural Engineers World Congress*, Bangalore, 2007).

Disc. 104-S58/From the September-October 2007 *ACI Structural Journal*, p. 611

Investigation of Deep Beams with Various Load Configurations. Paper by Michael D. Brown and Oguzhan Bayrak

Discussion by Dipak Kumar Sahoo, Bhupinder Singh, and Pradeep Bhargava

Research Scholar, Indian Institute of Technology, Roorkee, India; Assistant Professor, Indian Institute of Technology; and Professor, Indian Institute of Technology

The authors are to be complimented for their comprehensive and elaborate investigation of the behavior of deep beams under various load configurations. In the context of the investigation, the authors would like to respond to the following issues:

1. At the outset, attention is drawn to what seem to be printing errors in the 7th column of Table 1. The south reaction for Specimen UL-0-8.5 should be 204 kN (45.9 kip) instead of 2040 kN (458.6 kip) and that for Specimen CL-8.5-0 should be 124 kN (27.9 kip) instead of 1240 kN (278.8 kip).

2. For a more realistic assessment and comparison of the test results, normalized ultimate load (ultimate load per unit concrete strength), normalized cracking load (cracking load per unit concrete strength), and effective transverse reinforcement ratio calculated on the basis of the corrected Eq. (A-4) of ACI 318-05, Appendix A, have been tabulated in Table A. Keeping in mind that the strut efficiency is not expected to significantly vary with concrete strengths in the range of 16.3 to 22.3 MPa (2364.1 to 3234.3 psi) (Table 1), the following observations are made with respect to the normalized loads of Table 3:

a. Among the specimens with distributed loading, the ascending order based on ultimate strengths with reference to ACI-STM provisions for strut efficiency factors ought to be

$$UL-0-0 < UL-17-0 < UL-17-17 = UL-0-8.5 = UL-8.5-0a = UL-8.5-0b$$

The order, as seen in Table 1 and Fig.7, is

$$UL-0-8.5 < UL-0-0 < UL-17-17 < UL-8.5-0b < UL-17-0 < UL-8.5-0a$$

The order, as per the normalized ultimate loads presented in Table 3, is

$$UL-0-0 < UL-0-8.5 < UL-17-17 \approx UL-8.5-0b \approx UL-17-0 < UL-8.5-0a$$

The authors may like to address this inconsistency in specimen behavior.

b. A comparison between Specimens CL-0-0 and CL-8.5-0 shows that normalized ultimate load and normalized cracking load of the former having no web reinforcement are significantly higher than those of the latter satisfying web reinforcement requirements of Eq. (A-4), in ACI 318-05, Appendix A.¹ The authors have attributed this aberration to the large amount of scatter usually associated with results of shear behavior of concrete beams. The ratios of cracking load to ultimate load for Specimens CL-0-0 and CL-8.5-0, however, are 0.89 and 0.51, respectively (Fig. 7). The relatively lower ratio of 0.51 in the case of Specimen CL-8.5-0 indicates that web reinforcement has significantly improved the post-cracking load-carrying capacity of this specimen.

c. On the basis of the observed shear behavior of Specimens UL-0-0 and UL-0-8.5, the authors state that the horizontal shear reinforcement did not positively affect the shear strength of the specimens, and the large variation in

Table A—Normalized ultimate and cracking loads

Specimen ID	Concrete strength, MPa (psi)	Effective transverse reinforcement ratio, as per ACI 318-05, Eq. (A-4) $\left[= \sum \frac{A_{si}}{b_s s_i} \sin \alpha_i \right]$	Effective transverse reinforcement ratio (corrected) $\left[= \sum \frac{A_{si}}{b_s s_i} \sin^2 \alpha_i \right]$	Normalized ultimate load, kN/MPa (lb/psi)	Normalized cracking load, kN/MPa (lb/psi)
UL-8.5-0a	16.8 (2440)	0.0031	0.0022	56.9 (88.3)	17 (26.4)
UL-8.5-0b	18.2 (2640)	0.0031	0.0022	46.4 (72)	17.1 (26.5)
UL-0-0	22.3 (3230)	0	0	36.6 (56.8)	16.7 (25.9)
UL-0-8.5	18.2 (2640)	0.0031	0.0022	41.5 (64.4)	25.3 (39.3)
UL-17-17	18.3 (2660)	0.0031	0.0022	46.1 (71.5)	20.4 (31.7)
UL-17-0	18.3 (2660)	0.0016	0.0011	46.5 (72.2)	20.1 (31.2)
2C-8.5-0	22.1 (3210)	0.0031	0.0022	33.3 (51.7)	8.4 (13)
2C-0-0	22.1 (3210)	0	0	24.1 (37.4)	13.8 (21.4)
CL-8.5-0	17.8 (2580)	0.0034	0.0024	26.7 (41.4)	13.6 (21.1)
CL-0-0	16.3 (2370)	0	0	34.5 (53.5)	22.6 (35.1)

ultimate strength between these two specimens is ascribed to the differences in concrete strengths. The ultimate loads reported for Specimens UL-0-0 and UL-0-8.5 in Table 1 are 817 and 755 kN (184 and 170 kip), respectively, but when these loads are interpreted in terms of normalized ultimate loads, the corresponding values for Specimens UL-0-0 and UL-0-8.5, as reported in Table A, are 36.6 and 41.5 kN/MPa (56.8 and 64.4 lb/psi), respectively, which clearly reflect the influence of horizontal reinforcement on the shear strength of the specimens. Kong et al.¹¹ have reported that, depending on span-depth ratio L/D and shear span-depth ratio a/D , both vertical as well as horizontal web reinforcement influence the load-carrying capacity of deep beams.

3. It is appreciated that reinforcement will not have a significant influence on diagonal cracking load. Because, prior to cracking, shear is resisted by concrete alone, the diagonal cracking load should be dependent on the crushing strength of concrete. With reference to the data in Fig. 8, although the concrete crushing strength of Specimen CL-0-0 is 26% less than that of Specimen 2C-0-0, the former has 21% higher diagonal cracking load compared with the latter.

4. It would be instructive if the authors could clearly identify which of the following failure modes mentioned in the paper correspond to which of the beams used in their investigation: a) diagonal tension; b) crushing of concrete; and c) splitting failure of the strut.

5. Calculation of effective transverse reinforcement requirement and the minimum strut width for a diagonal strut depends on the inclination of the diagonal strut that, in turn, depends on the size of the bearing plates. Therefore, the authors may like to indicate the size of the bearing plates used at the loading points.

REFERENCES

11. Kong, F.-K.; Robins, P. J.; and Cole, D. F., "Web Reinforcement Effects on Deep Beams," ACI JOURNAL, *Proceedings* V. 67, No. 12, Dec. 1970, pp. 1010-1017.

AUTHORS' CLOSURE

The authors thank the discussers for their interest in the paper and critical evaluation of the work presented therein. The authors would like to provide answers for or comment on each one of the points raised by the discussers using the same reference/numbering scheme:

1. The discussers are correct. The errors they have indicated are typographical.

2. The author's are unaware of any lack of realism in the analysis of the data as presented in the paper.

a. It should be noted that the lists of specimens based on the actual failure loads and the normalized failure loads

mentioned by the discussers differ only in the order of the two weakest specimens. The authors are not aware of any inconsistency among the specimens. As indicated in the paper, the authors suggest that only small amounts of transverse reinforcement are necessary to enhance the failure loads of the specimens. Hence, specimens without transverse reinforcement failed at loads less than those with transverse reinforcement. That point is evident in either of the two lists of specimens presented by the discussers.

b. Specimen CL-8.5-0 failed at an ultimate load less than Specimen CL-0-0. The authors are unaware of the basis for the discussers' claim that Specimen CL-8.5-0 had a "significantly improved" post-cracking strength.

c. The greatest shear span-depth ratio of the specimens tested by Kong et al.¹¹ was 0.7. This value is much smaller than any of the specimens tested by the authors. Due to dissimilarity in the specimens, it is unclear how to compare the differing conclusions regarding the effectiveness of horizontal reinforcement. It should be noted, however, that the uniformly loaded specimen with only horizontal web reinforcement (UL-0-8.5) ranked near the weakest specimen in either of the discussers' lists in the previous comment. These results indicate that horizontal web reinforcement appears to be less beneficial than vertical web reinforcement.

3. The authors are unclear as to the point the discussers have raised. The cracking of concrete is related to its tensile strength rather than its compressive strength. The relationship between those two types of strength is approximate at best. The authors did not measure the tensile strength of the concrete as part of this study; thus, no analysis of the relationship between cracking load and tensile strength can be made.

4. It should be noted that the authors consider diagonal tension and splitting failure of the strut to be a single failure mechanism. Based on the photos presented in the paper, crushing of concrete is clearly visible in Specimens UL-17-0, UL-805-0a, and UL-80.5-0b. All other specimens failed through splitting of the strut.

5. As described in the original paper, the bearing plates were 6 x 6 in. (152 x 152 mm) at the north reaction and 6 x 8 in. (152 x 203 mm) at the south reaction. For specimens subjected to uniform loading, the loading plates were 3.5 in. (89 mm) in length. There was a 0.5 in. (13 mm) gap between adjacent plates. For specimens subjected to a single concentrated load, the bearing plate at the loading point was 8 in. (203 mm) in length. For specimens subjected to a pair of concentrated loads, the bearing plates were 6 in. (152 mm) in length. All bearing plates covered the full width of the beam specimens.

Disc. SP-246-10/From ACI Special Publication 246, *Structural Implications of Shrinkage and Creep*, p. 167

Effect of Shrinkage on Short-Term Deflections of Reinforced Concrete Beams and Slabs. Paper by Peter H. Bischoff and Ryan D. Johnson

Discussion by Gintaris Kaklauskas, Viktor Gribniak, and Darius Bacinskas

Professor, Head of Department, Vilnius Gediminas Technical University (VGTU), Vilnius, Lithuania; Researcher, VGTU; and Associate Professor, VGTU

The authors are to be congratulated for raising an important, but unjustly neglected, issue. In general practice, effects of shrinkage and creep are taken into account in prestress loss and/or long-term deformation analysis. Even at first loading, however, free shrinkage strain of concrete may be of such

magnitude that well exceeds the cracking strain. Due to restraining action of reinforcement, shrinkage-induced tension stresses in concrete may significantly reduce crack resistance and increase deformations of reinforced concrete (RC) members subjected to short-term loading. Most of the

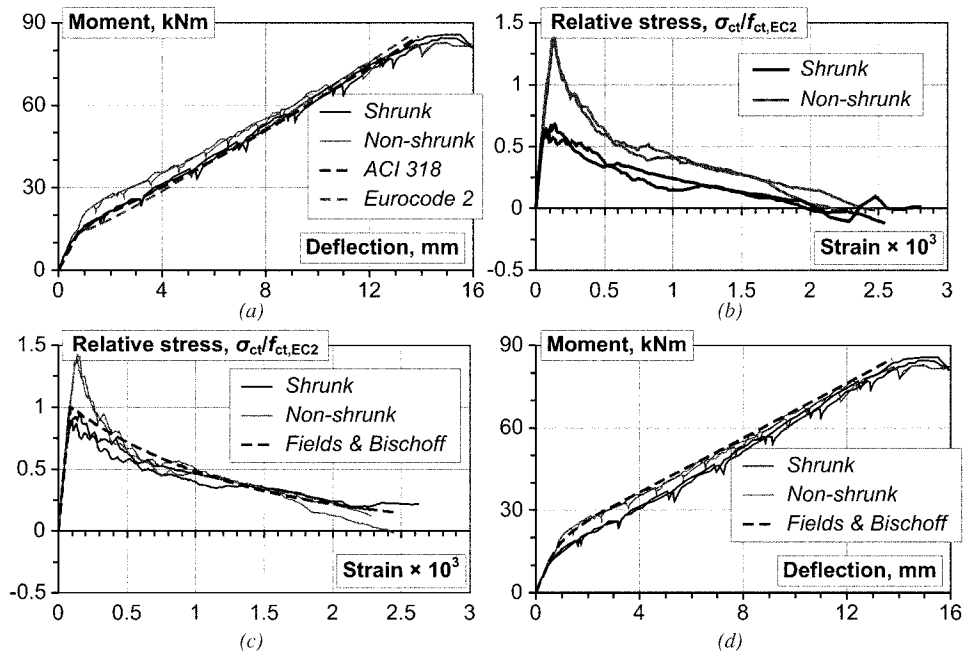


Fig. A—Shrinkage effect on deformation behavior of reinforced concrete beams.

techniques, however, do not take into account these effects in the short-term analysis.

In a series of publications, the first author and his associates have shown influence of shrinkage effect on tension stiffening and deformations of RC members subjected to short-term axial tension. Bischoff has proposed three analytical techniques based on load sharing and tension stiffening strain concepts. Using test data of shrunk RC tension members, Fields and Bischoff⁴ have derived a tension-stiffening stress-stress relationship free of shrinkage effects. Therefore, the paper under discussion dealing with bending members was a logical continuation of the research. The proposed analytical technique as well as new experimental data is a significant contribution to the state of the art of the issue.

The authors have reported results on tests of four RC beams with identical nominal geometrical parameters and cast from the same batch of concrete. One couple of the beams was protected from shrinking and tested at 14 days, whereas the second couple after 14 days of wet curing was exposed to drying condition and tested at 62 days. The test moment-deflection diagrams are shown in Fig. A(a) along with the analysis results performed by the ACI 318-05¹ and Eurocode 2¹³ techniques. The analysis was based on the reported cylinder strength of concrete. As shown in Fig. A(a), the code techniques accurately predicted the behavior of shrunk beams, whereas deflections of nonshrunk beams were overestimated. This suggests that the codes indirectly assess the effect of shrinkage.

Applicability of code methods is limited to simple cases of loading and structural shapes. A simple approach, extensively used in numerical modeling, is based on a smeared crack model and use of a stress-strain relationship of cracked tensile concrete. Stress in the concrete is taken as the combined stress due to tension stiffening and tension softening, collectively called the tension stiffening. Most the tension stiffening relationships were derived in a straightforward manner from tensile tests of RC members.⁴ Kaklauskas and Ghaboussi¹⁴ have proposed a method for deriving tension

stiffening relationships from test data of flexural RC members. This method is based on plane section hypothesis and employs moment-curvature or moment-average strain (at any layer) diagrams. Using the equilibrium equations, the stress-strain (tension stiffening) relationships are computed incrementally for the extreme fiber of tensile concrete. In this inverse approach, the previously computed portions of the stress-strain relationship at each load increment are used to compute the current increments of the stress-strain relationship.

In present analysis, moment-curvature diagrams were obtained from the test moment-deflection relationships shown in Fig. A(a). The conversion error due to the disregard of shear effects was insignificant, as the beams were tested under a four-point bending scheme. Tension stiffening relationships derived by the aforementioned method are shown in Fig. A(b) with the normalized stresses where the tension strength is according to Eurocode 2.¹³ Though a good match between the curves of the twin specimens was obtained, disagreement for the shrunk and nonshrunk beams was significant. The shrunk beams have shown much less tension stiffening effect than the nonshrunk beams. The maximal stresses for the shrunk beams were well below the tension strength. The cracking resistance was reduced by the shrinkage-induced tension stresses in concrete.

The aforementioned differences were due to the coupling of tension stiffening with shrinkage in the shrunk beams. In this study, shrinkage effect was eliminated from the tension stiffening relationships. The analysis was based on the layer approach that combined the direct¹⁵ and the inverse¹⁴ techniques, assuming reverse (expansion) shrinkage strain. A free shrinkage strain was calculated by the Eurocode 2¹³ technique assuming normal indoor conditions.¹⁶ The computed tension stiffening relationships with eliminated shrinkage effects are shown in Fig. A(c). The relationships obtained from the shrunk and nonshrunk members have approached each other and most parts have practically coincided. Only small portions with maximal stresses (corresponding to the initiation of cracking) differed,

but they practically had little effect on overall load-deflection behavior of the beams. It should be noted that these curves were in good agreement with the tension stiffening relationship proposed by Fields and Bischoff⁴ (refer to Fig. A(c)). As noted, the latter was derived from tension RC members by eliminating shrinkage effect. It should be remembered that the shape of tension stiffening relationships may depend on a number of parameters such as reinforcement bar diameter and bond characteristics, reinforcement ratio and bar distribution, section height, and cover.

A load-deflection diagram calculated by the layered model¹⁵ using the relationship proposed by Fields and Bischoff⁴ along with the originally reported experimental data is shown in Fig. A(d). The calculated moment-deflection diagram well predicted deflections of the nonshrunken beams.

In deriving most tension-stiffening relationships, the shrinkage effect was neglected. Shrinkage may significantly change the shape of the tension-stiffening relationship. Therefore, future tests should either eliminate shrinkage or carry out shrinkage and associated creep recordings for subsequent numerical elimination of this effect.

REFERENCES

13. Comité Européen de Normalisation, "Eurocode 2: Design of Concrete Structures—Part 1: General Rules and Rules for Buildings," CEN, Brussels, 2001, 230 pp.
14. Kaklauskas, G., and Ghaboussi, J., "Stress-Strain Relations for Cracked Tensile Concrete from RC Beam Tests," *Journal of Structural Engineering*, V. 127, No. 1, Jan. 2001, pp. 64-73.
15. Kaklauskas, G., "Flexural Layered Deformational Model of Reinforced Concrete Members," *Magazine of Concrete Research*, V. 56, No. 10, Dec. 2004, pp. 575-584.
16. Gribniak, V.; Kaklauskas, G.; and Bacinskas, D., "Shrinkage in Reinforced Concrete Structures: A Computational Aspect," *Journal of Civil Engineering and Management*, V. 14, No. 1, Mar 2008, pp. 49-60.

AUTHORS' CLOSURE

Interest expressed in the authors' paper is appreciated and the need to consider shrinkage and creep effects is reiterated in the discussion. The discussers go on to compare the authors' test results with design approaches used by ACI 318-05 and Eurocode 2, followed by a discussion of numerical modeling and development of a stress-strain relationship for cracked concrete that was originally introduced by Scanlon^{17,18} to account for tension stiffening of concrete. The observed correlation between tension stiffening results from axial tension members and flexural members is encouraging.

Tension stiffening in beams is controlled by the cracking moment, and member stiffness is reduced when a lower cracking moment is used in either the ACI 318-05 or Eurocode 2 approaches for computing deflection. Hence, accurate prediction of deflection is dependent on having the correct cracking moment.⁶ The cracking moment depends on the rupture modulus f_r of the concrete, and the authors' control tests gave a measured value of f_r equal to 5.2 MPa (750 psi) (corresponding to $0.78\sqrt{f'_c}$ MPa [$113.1\sqrt{f'_c}$ psi]) that was 25% greater than the ACI computed value of $0.62\sqrt{45} = 4.2$ MPa ($7.5\sqrt{6500} = 600$ psi). Development of tensile stresses from restraint to shrinkage probably reduced the apparent cracking stress to a value close to the ACI computed value, which is the reason why the discussers found that the code techniques gave a fairly reasonable

response prediction for the members that were allowed to shrink. Similar reasoning explains why the deflection response of the beams without any shrinkage restraint would be overestimated.

Code values for the rupture modulus represent a lower bound on tensile strength, and f_r can vary anywhere from $0.62\sqrt{f'_c}$ to $1.0\sqrt{f'_c}$ MPa ($7.5\sqrt{f'_c}$ to $12.0\sqrt{f'_c}$ psi).⁸ Hence, the fact that the observed cracking moment in the preshrunk beams corresponded to the ACI computed value is fortuitous. The first author of the paper has often carried out tests with concrete having a measured rupture modulus closer to $0.62\sqrt{f'_c}$ ($7.5\sqrt{f'_c}$) and, in this instance, the code approach would have underestimated member deflection of beams allowed to shrink before loading because the experimental (restrained) cracking moment would then be less than the ACI computed value.⁶

Despite the apparently good fit using either the ACI or Eurocode 2 approach for computing the response of the two beams that were allowed to shrink prior to loading (Fig. A(a)), the discussion fails to reconcile the fact that the measured response of these beams actually crosses over the I_{cr} response because of shrinkage (refer to Fig. 5 of the paper). Both the ACI and Eurocode 2 response gradually approach (but never cross) the I_{cr} response as tension stiffening decreases under increasing load. The effect of having the member response cross over the bare bar response is much easier to observe in axial tension members (Fig. 2 of the paper) and an explanation of this phenomenon constitutes one of the main messages in the paper. While the lower cracking moment that results from restraint to shrinkage is easily taken into account when computing deflection,⁶ the corresponding shift in the I_{cr} response is less well understood and most often ignored for this reason.

Tension stiffening represents tension carried by the concrete between cracks and is characterized by the difference between the measured member response and I_{cr} response, as shown in Fig. 5 for the four beams tested. Based on this observation, the beams that are allowed to shrink will appear to exhibit less tension stiffening unless the I_{cr} response is shifted over to the right (away from the member response). In fact, tension stiffening becomes negative once the member response crosses over the I_{cr} response and indicates that the concrete in the tensile zone is in compression, which of course is ridiculous. Figure A(c) from the discussion confirms there is little difference in tension stiffening between beams with or without shrinkage as long as the analysis takes shrinkage into account. Hence, any discrepancies or conflicting results that are sometimes observed between different research programs could well arise from failure to consider shrinkage effects; further work is needed in this area as pointed out in the discussion.

REFERENCES

6. Scanlon, A., and Bischoff, P., "Shrinkage Restraint and Loading History Effects on Deflection of Flexural Members," *ACI Structural Journal*, V. 105, No. 4, July-Aug. 2008. (Publication information updated since publication of SP-246 and is presented herein for reference).
17. Scanlon, A., "Time-Dependent Deflections of Reinforced Concrete Slabs," PhD thesis, University of Alberta, Edmonton, AB, Canada, 1971.
18. Scanlon, A., and Murray, D. W., "Time-Dependent Reinforced Concrete Slab Deflections," *Journal of the Structural Division*, ASCE, V. 100, No. ST9, Sept. 1974, pp. 1911-1924.